



## OPEN ACCESS

EDITED BY  
Benedetta Mattei,  
University of L'Aquila, Italy

REVIEWED BY  
Hongwei Guo,  
Southern University of Science and  
Technology, China  
Benoit Landrein,  
UMR5667 Laboratoire Reproduction et  
Développement des Plantes (RDP), France

\*CORRESPONDENCE  
Danny Geelen  
danny.geelen@ugent.be

SPECIALTY SECTION  
This article was submitted to  
Plant Proteomics and Protein Structural  
Biology,  
a section of the journal  
Frontiers in Plant Science

RECEIVED 11 March 2022  
ACCEPTED 27 July 2022  
PUBLISHED 08 September 2022

CITATION  
Lardon R, Trinh HK, Xu X, Vu LD,  
Van De Cotte B, Pernisová M, Vanneste S,  
De Smet I and Geelen D (2022) Histidine  
kinase inhibitors impair shoot regeneration  
in *Arabidopsis thaliana* via cytokinin  
signaling and SAM patterning determinants.  
*Front. Plant Sci.* 13:894208.  
doi: 10.3389/fpls.2022.894208

COPYRIGHT  
© 2022 Lardon, Trinh, Xu, Vu,  
Van De Cotte, Pernisová, Vanneste,  
De Smet and Geelen. This is an open-  
access article distributed under the terms  
of the [Creative Commons Attribution  
License \(CC BY\)](https://creativecommons.org/licenses/by/4.0/). The use, distribution or  
reproduction in other forums is permitted,  
provided the original author(s) and the  
copyright owner(s) are credited and that  
the original publication in this journal is  
cited, in accordance with accepted  
academic practice. No use, distribution or  
reproduction is permitted which does not  
comply with these terms.

# Histidine kinase inhibitors impair shoot regeneration in *Arabidopsis thaliana* via cytokinin signaling and SAM patterning determinants

Robin Lardon<sup>1</sup>, Hoang Khai Trinh<sup>1,2</sup>, Xiangyu Xu<sup>3,4</sup>,  
Lam Dai Vu<sup>3,4</sup>, Brigitte Van De Cotte<sup>3,4</sup>, Markéta Pernisová<sup>5,6</sup>,  
Steffen Vanneste<sup>1,3,4,7</sup>, Ive De Smet<sup>3,4</sup> and Danny Geelen<sup>1\*</sup>

<sup>1</sup>HortiCell, Department of Plants and Crops, Faculty of Bioscience Engineering, Ghent University, Ghent, Belgium, <sup>2</sup>Biotechnology Research and Development Institute, Can Tho University, Can Tho, Vietnam, <sup>3</sup>Department of Plant Biotechnology and Bioinformatics, Faculty of Sciences, Ghent University, Ghent, Belgium, <sup>4</sup>Center for Plant Systems Biology, VIB, Ghent, Belgium, <sup>5</sup>Mendel Centre for Plant Genomics and Proteomics, Central European Institute of Technology (CEITEC), Masaryk University, Brno, Czechia, <sup>6</sup>Laboratory of Functional Genomics and Proteomics, Faculty of Science, National Centre for Biomolecular Research, Masaryk University, Brno, Czechia, <sup>7</sup>Lab of Plant Growth Analysis, Ghent University Global Campus, Incheon, South Korea

Reversible protein phosphorylation is a post-translational modification involved in virtually all plant processes, as it mediates protein activity and signal transduction. Here, we probe dynamic protein phosphorylation during *de novo* shoot organogenesis in *Arabidopsis thaliana*. We find that application of three kinase inhibitors in various time intervals has different effects on root explants. Short exposures to the putative histidine (His) kinase inhibitor TCSA during the initial days on shoot induction medium (SIM) are detrimental for regeneration in seven natural accessions. Investigation of cytokinin signaling mutants, as well as reporter lines for hormone responses and shoot markers, suggests that TCSA impedes cytokinin signal transduction via AHK3, AHK4, AHP3, and AHP5. A mass spectrometry-based phosphoproteome analysis further reveals profound deregulation of Ser/Thr/Tyr phosphoproteins regulating protein modification, transcription, vesicle trafficking, organ morphogenesis, and cation transport. Among TCSA-responsive factors are prior candidates with a role in shoot apical meristem patterning, such as AGO1, BAM1, PLL5, FIP37, TOP1ALPHA, and RBR1, as well as proteins involved in polar auxin transport (e.g., PIN1) and brassinosteroid signaling (e.g., BIN2). Putative novel regeneration determinants regulated by TCSA include RD2, AT1G52780, PVA11, and AVT1C, while NAIP2, OPS, ARR1, QKY, and aquaporins exhibit differential phospholevels on control SIM. LC-MS/MS data are available via ProteomeXchange with identifier PXD030754.

## KEYWORDS

phosphoproteomics, kinase inhibitors, cytokinin signaling, shoot regeneration, organogenesis

## Introduction

Reversible protein phosphorylation is a post-translational modification (PTM) with a widespread regulatory function in biological systems, as it can alter protein activity, structure, stability, subcellular localization and interactions with other proteins (Park et al., 2012; van Wijk et al., 2014). In plants, phosphorylation is involved in virtually all processes, from growth and development to immunity and abiotic stress resistance, largely due to its role in signal transduction and fine-tuning metabolism (Wang et al., 2007; Park et al., 2012). This is also reflected in the abundance and diversity of kinases and phosphatases in the genome of *Arabidopsis thaliana* (Wang et al., 2007; van Wijk et al., 2014). In particular the receptor-like protein kinases (RLKs), mitogen-activated protein kinase kinase kinases (MKKKs), calcium-dependent protein kinases (CDPKs) and type 2C protein phosphatases (PP2Cs) constitute large families in this model plant (Wang et al., 2007). Phosphate groups can be transferred to the side chains of several amino acids in a peptide, but the most common ones are serine (Ser) and threonine (Thr), followed by tyrosine (Tyr; Park et al., 2012). These are examples of O-phosphorylation, but in rare cases N atoms in histidine (His), lysine (Lys) or arginine (Arg) residues can be phosphorylated as well. Although less common and less stable than phosphoesters, phosphohistidines act as intermediates in two-component signaling relays that are key for environmental adaptation in plants (Ross, 2007). These systems are built around histidine kinases, of which there are at least eight in *Arabidopsis*, including two ethylene receptors (ETHYLENE RESPONSE 1 (ETR1) and ETHYLENE RESPONSE SENSOR 1 (ERS1)), one putative osmosensor (ARABIDOPSIS HISTIDINE KINASE 1 (AHK1)), three cytokinin receptors (AHK2, AHK3 and AHK4/CYTOKININ RESPONSE 1 (CRE1)/WOODEN LEG (WOL)) and two receptors whose function remains unclear (CYTOKININ INSENSITIVE 1 (CKI1) and CKI2/AHK5; Hwang et al., 2002; Nongpiur et al., 2012).

Plant regeneration through *de novo* organogenesis refers to the reconstruction of body parts upon wounding or *in vitro* cultivation, which is key for survival and serves a plethora of biotechnological applications (Ikeuchi et al., 2016, 2019). For example, adventitious roots or shoots can be formed from excised tissue explants for mass clonal propagation and genetic engineering requires regeneration of intact plants from transformed protoplasts (Lardon and Geelen, 2020). These processes rely on plant hormones, such as auxin, cytokinin (CK), brassinosteroids (BR), jasmonic acid (JA), etc. Especially the ratio of auxin to CK determines the identity of regenerating organs, because auxins promote root development and cytokinins stimulate shoot formation (Motte et al., 2014b). Notably, many hormone signal transduction pathways involve phosphorylation. A prime example of this is CK, which is perceived by a two-component His-Asp phosphorelay, that starts with the activation of one of three hybrid receptors (AHK2-4; Schaller et al., 2015; Kieber and Schaller, 2018). Binding of CK to the

extracytosolic CHASE domain triggers autophosphorylation of a conserved His residue and transfer of the phosphate to an Asp residue in the receiver domain. From here, it is passed on to ARABIDOPSIS HISTIDINE PHOSPHOTRANSFER (AHP) proteins, that move into the nucleus and activate ARABIDOPSIS RESPONSE REGULATORS (ARRs). B-type ARR contains a MYB-like DNA-binding domain and induce a transcriptional response, while A-type ARRs induced by the former impose a negative feedback on the signal through competition (Kieber and Schaller, 2018). Several auxin biosynthetic enzymes, PIN efflux carriers and AUXIN RESPONSE FACTORS (ARFs) are regulated by phosphorylation as well (Tan et al., 2021). Moreover, BRs are required for regeneration, as they control organ boundaries in the shoot apical meristem (SAM; Bell et al., 2012; Gendron et al., 2012), they mediate cell division in the root quiescent center (González-García et al., 2011; Lozano-Elena et al., 2018) and biosynthetic mutants show reduced callus growth and shoot induction (Cheon et al., 2010). In the presence of BR, BRASSINOSTEROID INSENSITIVE 1 (BRI1) and BRI1 ASSOCIATED KINASE 1 (BAK1) heterodimerize and initiate a cytoplasmic phosphorylation cascade that causes degradation of BRASSINOSTEROID INSENSITIVE 2 (BIN2; a GSK3/SHAGGY-like kinase) and increased levels of dephosphorylated BRASSINAZOLE RESISTANCE 1 (BZR1) and BRI1-EMS-SUPPRESSOR 1 (BES1). These transcription factors (TFs) induce a transcriptional response that controls cell elongation and division, underscoring the central role of phosphorylation in hormone-regulated regeneration (Cheon et al., 2010; Lozano-Elena et al., 2018).

Besides hormone signaling, phospho-regulation of organogenesis is mediated by specific kinases and phosphatases. For instance, the leucine-rich repeat (LRR)-RLK CLAVATA1 (CLV1) perceives CLV3 in a feedback loop with WUSCHEL (WUS), a TF that determines the balance between proliferation and differentiation in the SAM (Wang et al., 2007; Somssich et al., 2016). CLV1 can be dephosphorylated by KINASE ASSOCIATED PROTEIN PHOSPHATASE (KAPP) and it acts upstream of the PP2C phosphatases POLTERGEIST (POL) and POL-LIKE 1 (PLL1), which are essential for SAM establishment (Yu et al., 2003; Wang et al., 2007; Song et al., 2020). The CLV1 homologs BARELY ANY MERISTEM (BAM) 1–3 also regulate stem cell maintenance in the shoot, but they have broad expression patterns and their function is opposite to that of CLV1 (DeYoung et al., 2006). Other LRR-RLKs that play a role in regeneration include STRUBBELIG (SUB), which controls cell division in the SAM (Chevalier et al., 2005), RECEPTOR-LIKE PROTEIN KINASE 1 (RPK1), a potential abscisic acid receptor that responds to abiotic stresses and underlies natural variation in shoot regeneration from root explants (Motte et al., 2014a) and SOMATIC EMBRYOGENESIS RECEPTOR-LIKE KINASES (SERKs), that are specifically induced during somatic embryogenesis and enhance the process when overexpressed (Méndez-Hernández et al., 2019). Note that BAK1 is a member of the SERK family that also takes part in a developmental pathway encompassing the MKKK YODA (YDA;

Wang et al., 2007). In short, SERKs interact with ERECTA (ER) family RLKs and possibly BR signaling kinases [e.g., SHORT SUSPENSOR (SSP) and the BRI1 target BSK1] found downstream or parallel of the ER-SERK complex in the phosphorylation of YDA, which can also occur directly by BIN2 and controls a MAPK cascade composed of MKK4 and MKK5 upstream of MPK3 and MPK6 to mediate embryonic patterning, inflorescence architecture and stomata formation (Kim et al., 2012; Meng et al., 2013; Li et al., 2019; Neu et al., 2019). This cascade is also activated by auxin *via* a non-canonical pathway involving transmembrane kinases (TMKs) 1 and 4 to regulate cell division during lateral rooting (Huang et al., 2019b). MKK7 and PINOID (PID) further control auxin responses by fine-tuning polar transport (Wang et al., 2007). Additionally, the RLK ARABIDOPSIS CRINKLY 4 (ACR4), involved in founder cell specification during lateral root initiation and expressed in the SAM during embryogenesis, has been proposed as a marker for acquisition of organogenic competence (De Smet et al., 2008; Motte et al., 2014b).

In an approach termed chemical genetics, small organic molecules that perturb specific biological processes are used to study a phenotype of interest (Blackwell and Zhao, 2003; Mccourt and Desveaux, 2010). The advantage of this strategy over reverse mutational analysis is that it overcomes functional redundancy and lethality, while enabling temporal and dosage control (Hicks and Raikhel, 2012, 2014; Xuan et al., 2013). Disadvantages, however, include possible off-target effects, poor uptake, and metabolic conversion. In the context of phosphorylation, several compounds have been used to block the function of protein kinases. Examples of such kinase inhibitors are rapamycin, AZD8055, bikinin, olomoucine, 3,3',4',5-tetrachlorosalicylanilide (TCSA) and Closantel® (Papon et al., 2003; De Rybel et al., 2009; Sheremet et al., 2010; Van Leene et al., 2019). The TARGET OF RAPAMYCIN (TOR) is an evolutionary conserved Ser/Thr kinase that balances growth in response to nutrient availability and environmental stresses by modulation of protein synthesis (Ren et al., 2012; McCready et al., 2020). It is also involved in embryo development, meristem activation, auxin signaling, adventitious rooting and DNA methylation (Menand et al., 2002; Xiong et al., 2013; Deng et al., 2016, 2017; Zhu et al., 2020a). Notably, rapamycin depends on FKBP12 to block TOR function and reduced affinity for the plant FKBP12 homolog causes insensitivity of *Arabidopsis* seedlings to physiological concentrations of the compound (Menand et al., 2002; Ren et al., 2012). Nonetheless, hypoxia partially restores inhibition and there is substantial overlap in the phosphoproteome of cell cultures treated with rapamycin or the potent TOR inhibitor AZD8055 (Deng et al., 2016; Van Leene et al., 2019). Rapamycin also blocks glucose-induced root growth *via* the TOR kinase (Xiong et al., 2013). Bikinin inhibits GSK3-like kinases (e.g., BIN2; De Rybel et al., 2009) and olomoucine targets cyclin-dependent protein kinases, thereby blocking cell cycle progression and altering root morphology (Sheremet et al., 2010). TCSA and Closantel® inhibit bacterial histidine kinases and impede CK signaling in periwinkle cell cultures (Papon et al., 2003). In the

same system, these drugs hamper ethylene-induced alkaloid biosynthesis *via* ETR1 (Papon et al., 2004). In *Arabidopsis*, sensing of H<sub>2</sub>O<sub>2</sub> by AHK5 to integrate endogenous and environmental stimuli (e.g., darkness, ethylene, and nitric oxide) in stomatal guard regulation was blocked by TCSA (Desikan et al., 2008). Other phenotypic effects of TCSA and Closantel® in plants have not been investigated. These examples illustrate that Closantel® and TCSA target His kinase activities in plants. However, salicylanilide derivatives disrupt membrane integrity and long-term exposure causes toxic effects on cell growth (Papon et al., 2003).

Despite the abundance of evidence suggesting that regeneration depends on phosphorylation, comprehensive studies of phosphoproteome dynamics have been restricted to protoplast regeneration in moss and cell dedifferentiation in *Arabidopsis* (Chitteti and Peng, 2007; Wang et al., 2014b). This uncovered a variety of phosphopeptides involved in cell wall metabolism, cytoskeleton structure, signal transduction, transcriptional regulation, cell division and photosynthesis. Here, we explored the effect of three kinase inhibitors on shoot regeneration from root explants in *Arabidopsis thaliana* and optimized the application of TCSA for downstream analyses. We then examined how this compound interacts with cytokinin signaling by testing mutants and reporter lines. Finally, we exploited mass spectrometry (MS)-based shotgun proteomics to probe phosphoproteome changes upon TCSA treatment and identify phosphorylation events that govern *de novo* shoot organogenesis parallel or downstream of cytokinin perception.

## Materials and methods

### Plant materials and chemicals

Natural *Arabidopsis thaliana* (L.) Heynh. accessions Lp2-2, Kyoto, Kz-9, Sg-1, and Db-1 were obtained from the Nottingham *Arabidopsis* Stock Centre (NASC; N76636). Ws and Col-0 are descendants from seed stocks purchased at the Versailles *Arabidopsis* Stock Center (INRA; 530AV) and NASC (N76778). Cytokinin mutants *ahk2-5*, *cre1-2*, *ahk2-5 ahk3-7*, *ahk2-5 cre1-2*, *ahk3-7 cre1-2*, *ahk2-5 ahk3-7/AHK3 cre1-2* (Riefler et al., 2006), *ahk2-1*, *ahk3-1* (Nishimura et al., 2004; Jeon et al., 2010), *ahk2-2 ahk3-3* (Higuchi et al., 2004; Jeon and Kim, 2013), *ahp2-1* (CS860144), *ahp3* (CS660145), *ahp5-2* (CS860148), *ahp2-1 ahp3* (CS860151), *ahp2-1 ahp5-2* (CS860153), *ahp3 ahp5-2* (CS860155), *ahp2-1 ahp3 ahp5-2* (CS860161), *arr1-3* (CS6971; Jeon and Kim, 2013), *35S:ARR1-SRDX* (Heyl et al., 2008), and *ARR1* phosphomimic (*35S:ARR1<sup>D94E</sup> arr1-1*; Kurepa et al., 2014a) are all in Col-0 background and were described previously. Reporter lines carrying *proTCSn::GFP* and *proWUS::tdTom* in WT Col-0 and *ahk4* backgrounds were kindly provided by Markéta Pernisová (Masaryk University; Pernisova et al., 2018). *ProDR5::GFP* and *proSTM::GFP* were obtained from NASC (respectively N9361 and N68954).

Rapamycin and TCSA (3,3',4',5'-Tetrachlorosalicylanilide) were purchased from Fisher Scientific™ (respectively Catalog No. 15434849; CAS No. 53123–88-9, Catalog No. 10473741; CAS No. 1154-59–2) and Closantel® (5'-Chloro-4'-(4-chloro- $\alpha$ -cyanobenzyl)-3,5-diiodo-2'-methylsalicylanilide, N-[5-Chloro-4-(4-chloro- $\alpha$ -cyanobenzyl)-2-methylphenyl]-2-hydroxy-3,5-diiodobenzamide) was obtained from Sigma-Aldrich (Product No. 34093; CAS No. 57808–65-8). Kinase inhibitors were dissolved in DMSO (dimethyl sulfoxide) at a stock concentration of 10 mM and filter sterilized before addition to the SIM.

## Regeneration assays

The protocol for shoot regeneration from root explants was adapted from the work of [Valvekens et al. \(1988\)](#). Seeds were sterilized by exposure to chlorine gas for 4 h and sown on Gamborg B5 medium [3.1 g/l B5 salts including vitamins, 0.05% 2-(4-morpholino)-ethane sulfonic acid (MES), 2% (w/v) glucose and 0.7% agar at pH 5.8]. After vernalization at 5°C for 4 days, seedlings were grown under warm white fluorescent tungsten tubes ( $\sim 100 \mu\text{M m}^{-2} \text{ s}^{-1}$ ) at 21°C following a 14/10 h light/dark regime for 10 days. Next, 7 mm long root segments including the tip were excised and placed on CIM [B5 supplemented with 2.2  $\mu\text{M}$  2,4-dichlorophenoxy acetic acid (2,4-D) and 0.2  $\mu\text{M}$  kinetin] for 4 days. Finally, the explants were transferred to SIM [B5 supplemented with 5  $\mu\text{M}$  2-isopentenyl adenine (2-IP) and 0.86  $\mu\text{M}$  3-indole acetic acid (IAA)] and incubated for 21 days. Timed application of kinase inhibitors at this stage was achieved by transferring explants to new SIM plates supplemented with 10  $\mu\text{M}$  rapamycin, TCSA or Closantel® for the indicated periods [the concentration is based on experiments by [Desikan et al., 2008](#)]. Untreated controls were kept on the original plate. To score regeneration, pictures were taken using binoculars (6.3 $\times$ ) and the green area was determined in ImageJ. Further data processing and plot construction was done in R.

## Microscopy

Root explants were subjected to the regeneration protocol described above and harvested right before transfer to SIM (4dCIM), after 24 h on SIM (24hSIM), and after 28, 48, 72, and 120 h on SIM (28hSIM, 48hSIM, 72hSIM, and 120hSIM) following incubation on SIM supplemented with 10  $\mu\text{M}$  TCSA or an equal amount of DMSO between 24 and 28 h (24h-28h\_TCSA and 24h-28h\_mock). Slides were prepared with 150  $\mu\text{l}$  of Milli-Q water and for each combination of reporter line, treatment, and time, 6–12 explants were analyzed (1–6 non-overlapping segments were recorded per explant). Imaging was done at 10 $\times$  in CellSens using an Olympus IX81 fluorescence microscope powered by an X-cite® 120 LED Boost lamp coupled to an Olympus XM10. Exposures were manually set to 150 ms for *proTCSn::GFP* lines, 1 s for *proWUS::tdTom* lines and 500 ms for *proDR5::GFP* and

*proSTM::GFP* lines. For GFP measurements, a U-FCFP Fluorescence Filter Cube (BX3) was used (excitation filter: BP 425–445 nm, dichromatic mirror: DM 455 nm and emission filter: BP 460–510 nm) and for tdTom detection, a U-MWU2 Fluorescence Filter Cube (BX2/IX2) was applied (excitation filter: BP 330–385 nm, dichromatic mirror: DM 400 nm and emission filter: LP 420 nm). Corrected total cell fluorescence was determined in ImageJ by auto thresholding the image (using the “triangle white” method) to select the explant and then subtracting the mean background intensity multiplied by the explant area from the integrated density of pixels within the explant.

## Phosphoproteomics

Per sample, 200–300 seedlings were subjected to the shoot regeneration protocol described above. Instead of sampling individual root explants, however, plantlets were grown in a horizontal line and the lower 2 cm of all root systems was cut with a razor for transfer between media. Harvesting was done by flash freezing  $\sim 250$  mg of roots in liquid nitrogen before grinding in a Retch® mill for 1 min at 20 Hz, followed by 30 s at 30 Hz. Protein extraction, digestion, phosphopeptide enrichment and LC-MS/MS analysis were carried out according to [Vu et al. \(2016\)](#). First, Tris-HCl homogenization buffer (containing 50 mM Tris-HCl, 0.1 M KCl, 5 mM EDTA, 500 mM DTT, and 30% sucrose at pH 8.0), supplemented with 1 Protease Inhibitor Cocktail Tablet (Roche) and 1 PhosSTOP Phosphatase Inhibitor Cocktail Tablet (Roche) per 50 ml, was added to the samples. Debris was removed by sonication and centrifugation at 4°C and 2,500 g for 15 min. Next, proteins were precipitated by chloroform extraction and centrifuged, after which 20 ml methanol was added to mix with the aqueous phase in each tube. After another centrifugation, pellets were washed with 80% acetone and resuspended in 50 mM triethylammonium bicarbonate (TEAB) buffer containing 6 M guanidinium hydrochloride (pH 8.0). Cysteine alkylation was done by addition of Tris-(2-carboxyethyl) phosphine (TCEP, Pierce) and iodoacetamide (Sigma-Aldrich) in final concentrations of 15 and 30 mM, respectively, and the reaction was allowed to proceed for 15 min at 30°C (in the dark). Next, 2.5 mg of each sample was pre-digested using 1 aliquot of 10  $\mu\text{g}$  EndoLysC (Wako), while mixing for 2.5 h (in the dark). Samples were then diluted 8 $\times$  in 50 mM TEAB, followed by overnight digestion with trypsin (Promega Trypsin Gold; mass spectrometry grade). Both digestions occurred at 37°C using an enzyme-to-substrate ratio of 1% w/w. To stop digestion, samples were acidified to pH  $\leq 3.0$  with TFA, before desalination using SampliQ C18 SPE cartridges (Agilent) according to the manufacturer's guidelines. Subsequently, the digests were vacuum-dried and redissolved in loading solvent for enrichment of phosphopeptides using Ti-IMAC beads. After elution, samples were acidified, vacuum-dried and resuspended in acetonitrile solution for liquid chromatography on an Ultimate 3000 RSLC nano LC (Thermo Fisher Scientific). This was coupled in-line to a Q Exactive mass spectrometer (Thermo Fisher Scientific) operated in data-dependent, positive ionization

mode and using HCD collision to acquire MS/MS scans for the 10 most abundant precursor ions in each MS1 spectrum (Vu et al., 2016). The mass spectrometry proteomics data have been deposited to the ProteomeXchange Consortium via the PRIDE (Perez-Riverol et al., 2019) partner repository with the dataset identifier PXD030754.

Identification and quantification of (phospho) peptides from MS/MS spectra was done in MaxQuant (version 1.6.11.0; Supplementary Data 2; Cox and Mann, 2008; Tyanova et al., 2016a). Methionine oxidation, protein N-terminal acetylation and phosphorylation of S, T, and Y residues were chosen as variable modifications, and cysteine carbamidomethylation was included as fixed modification (with maximum five modifications per peptide). Trypsin was selected for digestion, allowing cleavage at lysine or arginine residues followed by proline, and up to 2 missed cleavages. Respective precursor mass tolerances of 20 and 4.5 ppm were used for the first and main search, intensity thresholds for MS1 and MS2 were set to 500, and DIA quantification and feature quantification methods were, respectively set to “Top fragments by annotation” and “Scan” (using the top three fragments and a top MS/MS intensity quantile of 0.8). DIA mass window factor, background subtraction quantile and factor were all set to 0, and DIA XGBoost sub sample was set to 0.65, with a binary logistic learning objective and minimum child weight of 3. Default values (in ppm) were used for other instrument settings. Database searches were done against a FASTA file with protein sequences for all predicted transcripts in *Arabidopsis thaliana* Ws-0, derived from the 19 Genomes Project (Gan et al., 2011). Decoy mode was kept at “Revert” and default parameters were used under the protein quantification, label-free quantification, and MS/MS analyzer tabs. An FDR filter of 1% was applied to peptide spectrum matches, protein identifications, and modification sites, and the “Match between runs” feature was used (with a match time window of 0.7 min, match ion mobility window of 0.05, alignment time window of 20 min, and alignment ion mobility of 1). The Phospho (STY)Sites.txt table produced by MaxQuant was uploaded in Perseus (version 1.6.10.50; Tyanova et al., 2016b) to remove potential contaminants and reverse hits. Also, rows were filtered to have a localization probability  $\geq 0.75$ , site multiplicities were expanded, and intensity values were  $\log_2$  transformed. Next, the data were uploaded in R for statistical analysis with the DEqMS package (see Supplementary Code; results are available in Supplementary Data 1; Zhu et al., 2020b).

## Gene set enrichment analysis

GSEA was performed with the ClueGO and CluePedia plugins for Cytoscape (Shannon et al., 2003; Bindea et al., 2009, 2013). All 522 genes corresponding to significantly deregulated phosphosites between TCSA and mock treatment on SIM (FDR  $\leq 0.05$ ) were uploaded in ClueGO and compared to a predefined reference set containing 25,386 Ensembl gene identifiers for *Arabidopsis thaliana* using a right-sided hypergeometric test and correcting for multiple tests according to Benjamini-Hochberg. Enriched GO Biological Process and Immune System Process terms (Ashburner et al., 2000;

The Gene Ontology Consortium, 2014), KEGG pathways (Kanehisa and Goto, 2000), PO Anatomy—Plant Structure, and PO Temporal—Plant Growth and Developmental Stage terms (Avraham et al., 2008) with FDR  $\leq 0.03$ ,  $5 \leq$  GO tree interval level  $\leq 12$ ,  $\geq 3$  associated genes, and  $\geq 5\%$  associated genes were retained (using all evidence codes). GO term fusion and grouping options were enabled, “Groups” was selected under visual style, and the connectivity threshold (kappa score) was set to 0.3. Grouping was based on kappa scores, using random colors, an initial group size of 1, and group merge percentages of 50% (terms/genes). Overview terms were defined by highest significance. The yFiles Organic Layout was used for network construction, and only genes from the input list mapping to enriched functional terms were included in the graph. The resulting network contains 75 functional terms (connected by 103 edges and divided into 16 groups), 194 genes, and 838 edges. Centrality parameters in the network (degree and betweenness) were calculated with CentiScaPe (Scardoni et al., 2009). A bar plot reflecting less stringent settings (FDR  $\leq 0.05$ ,  $5 \leq$  GO tree interval level  $\leq 15$ ,  $\geq 2$  associated genes, and  $\geq 5\%$  associated genes) is presented in Supplementary Figure 2, including 115 functional terms divided into 26 groups.

## Statistics and reproducibility

All experiments were performed once. In the regeneration assays, 24–30 explants were analyzed per combination of treatment and line, and 6–12 root segments were harvested for microscopic analysis. As the calculated green area and corrected total cell fluorescence were not normally distributed, non-parametric statistics were used. Global significance was assessed by Kruskal–Wallis tests and pairwise comparisons were based on Dunn’s tests or Wilcoxon rank sum tests (as explained in the figure captions). For the phosphoproteome analysis, five independent biological replicates were sampled for each of the three design points and two technical replicates were performed in each LC–MS/MS run. Only phosphosites detected in  $\geq 2$  samples for each treatment group were retained in the statistical analysis, and run effects were normalized by subtracting the median  $\log_2$  sample intensity. For DEqMS analysis, the minimum number of unique and razor peptides used for quantification of each phosphosite across samples was retrieved from the proteinGroups.txt table, and limma (Ritchie et al., 2015) was run in robust trend mode. Volcano plots and heatmaps were, respectively constructed with the EnhancedVolcano and ComplexHeatmap packages in R (Gu et al., 2016).

## Results

### Kinase inhibitors modulate shoot regeneration

Given the pivotal role of cytokinin perception and protein phosphorylation in *de novo* shoot organogenesis, we sought to

delineate the time window of critical phosphorylation events for regeneration by interfering with histidine kinases using TCSA and Closantel® (Papon et al., 2003, 2004). As a negative control, we included rapamycin, which has limited impact on plant development under physiological conditions because of structural divergence in the FKBP12 protein required to block TOR kinase activity (Menand et al., 2002; Li et al., 2012). Root explants of *Arabidopsis thaliana* (ecotype Wassilewskija; Ws) were subjected to a two-step protocol for shoot regeneration, in which they are pre-incubated on auxin-rich callus-induction medium (CIM) for 4 days, before transfer to cytokinin-rich shoot induction medium (SIM). After 21 days on SIM, the regeneration rate was scored by measuring the green area of explants. Initially, the impact of kinase inhibitors on shoot induction was assessed using broad application intervals: from 0 to 8 h, 0 to 24 h, 24 to 48 h, 48 to 72 h, 72 to 96 h, or during all 21 days on SIM (Figures 1A,B,E,F,I,J). Subsequently, we tested narrower treatment windows for each inhibitor, based on the results of the first screen (Figures 1C,D,G,H,K,L). Chemicals were applied at a concentration of 10 μM based on previous reports (Papon et al., 2003; Desikan et al., 2008) and an experiment showing that 10 μM TCSA yields the most specific reduction of regeneration in Ws, while balancing toxic off-target effects (Supplementary Figure 1).

We find that TCSA is detrimental to shoot regeneration, while Closantel® and rapamycin either have no effect or promote the process, depending on the time of application (Figure 1). Intriguingly, TCSA is most potent when applied during the first 4 days of SIM incubation, especially when applied in short intervals, as exposure from 0 to 24 h and 24 to 28 h yields the lowest regeneration rates and treatment from day 5 to day 21 on SIM even has a slightly positive influence (Figures 1A–D,M,N). An inverse trend is observed for Closantel®, which has no significant effects when applied for less than 24 h (Figures 1G,H,O) and promotes shoot regeneration when administered during the first 4 days of SIM incubation. The latter effect is strongest from 0 to 24 h (Figures 1E,F). Contrary to the reported lack of effects of rapamycin on vegetative growth (Menand et al., 2002), this compound enhances *in vitro* shoot formation in our experiments. This effect occurs at later application windows than observed for Closantel® (e.g., 44 to 48 h, 72 to 96 h or 0 to 21 days on SIM; Figures 1I–L,P), and hints at involvement of rapamycin-sensitive Ser/Thr kinases that negatively regulate *de novo* organogenesis. Note that rapamycin also promotes regeneration when administered in the initial 24 h. Overall, root explants are most susceptible to TCSA and Closantel® from 8 to 28 h on SIM, as the 0 to 8 h treatment does not have substantial effects on shoot regeneration. In particular, the data indicate that shoot regeneration is highly sensitive to a pulse of TCSA administered from 24 to 28 h on SIM, so this treatment was studied in subsequent analyses.

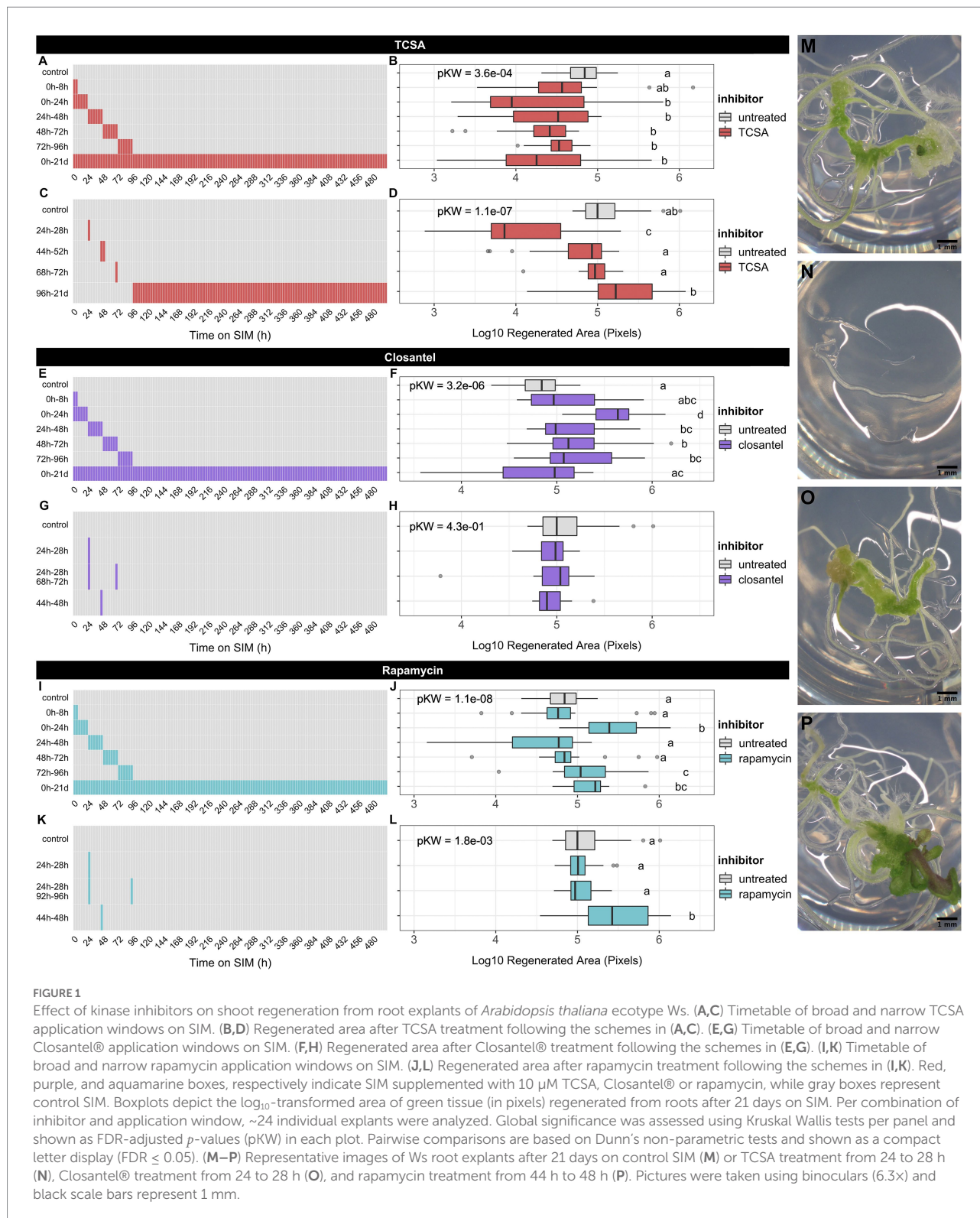
## Regeneration in natural accessions is differentially reduced by TCSA

Next, we assessed the robustness of TCSA effects by comparing regeneration rates in seven natural *Arabidopsis*

*thaliana* accessions after treatment with this inhibitor, using the same setup as before. We selected Columbia-0 (Col-0) and Wassilewskija (Ws) because they are commonly used genetic backgrounds and included five other accessions previously shown to have a high capacity for shoot regeneration (Lardon et al., 2020). Evaluating untreated explants of these strains after 21 days on control SIM shows that Col-0 regenerates poorly, while Ws and the other ecotypes are average to strong performers. For an optimal inhibitory effect on shoot organogenesis (Figures 1A–D), TCSA was applied to root explants from 24 to 28 h on SIM. In all accessions, regeneration is reduced by this pulse TCSA treatment, albeit with variable efficiency (Figure 2A). The absolute difference in regenerated area between control and TCSA-treated explants is largest in the best regenerating ecotypes (e.g., Db-1), but log-fold changes are higher in strains with average regeneration capacities (e.g., Ws). To verify the efficacy of the short pulse treatment across multiple accessions, TCSA was also applied during an extended interval from 24 to 48 h on SIM. While Col-0 explants show increased susceptibility to prolonged TCSA exposure, this treatment has little effect in accessions with a higher regenerative potential (Figure 2B). In conclusion, TCSA treatment from 24 to 28 h on SIM robustly inhibits shoot regeneration in various *Arabidopsis* ecotypes.

## TCSA interferes with cytokinin signaling

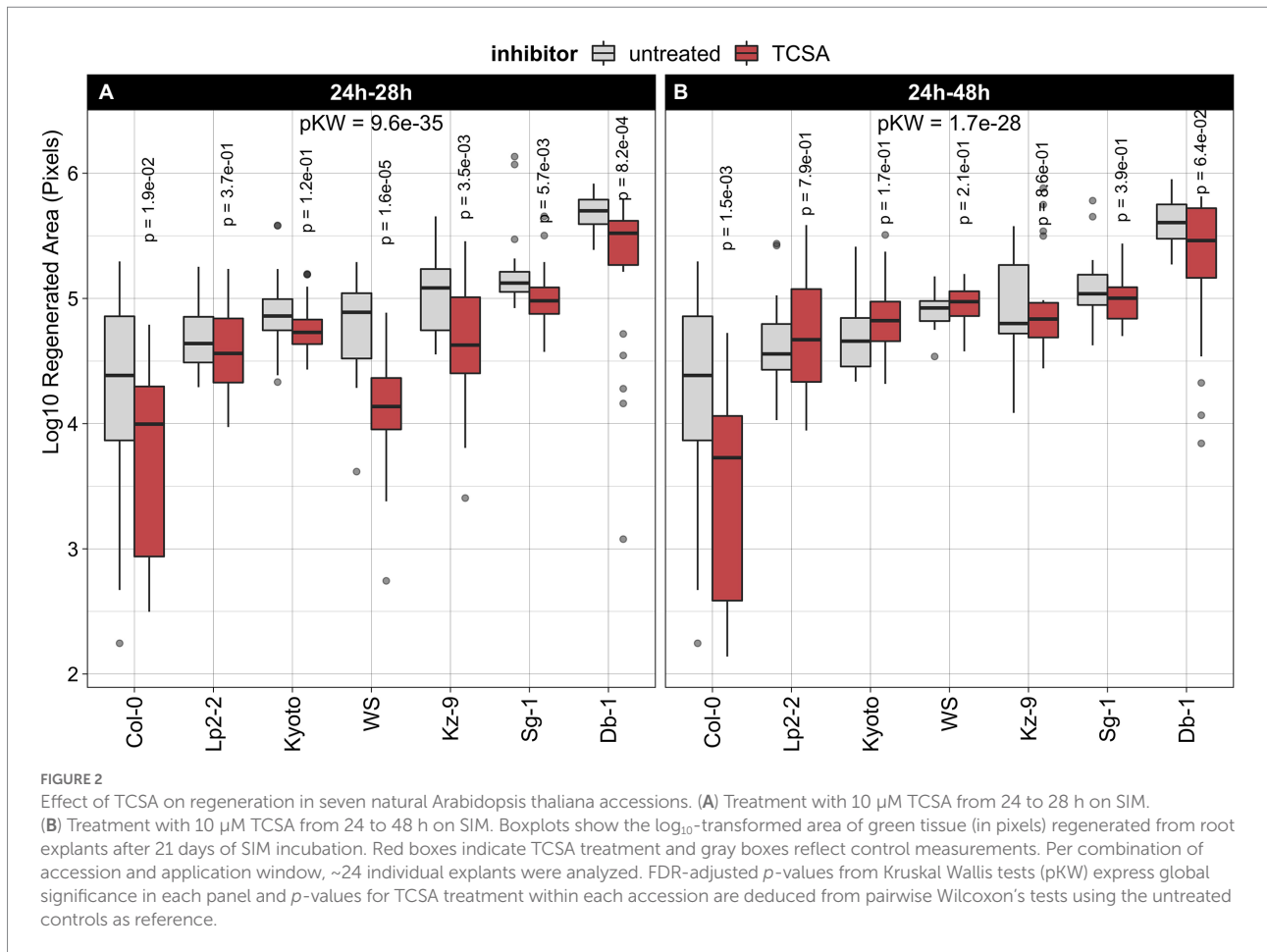
As the cytokinin signaling machinery operates *via* a His-Asp phosphorelay, it is a prime target for histidine kinase inhibitors in plants. To determine if TCSA affects shoot regeneration by specifically interfering with CK signaling, genetic interaction of TCSA with canonical CK receptors (AHKs) and downstream components (AHPs and ARR) was evaluated. Hereto, we applied TCSA from 24 to 28 h on SIM, and during the full 21-day incubation period (because most of the available mutants are in Col-0 background and this accession is susceptible to prolonged TCSA treatment; Figure 2). The area of regenerated shoot tissues in wild-type (WT) Col-0 explants declines progressively when extending the exposure to TCSA (Figures 3A,B,G,L). This trend is also apparent in most of the cytokinin mutants, but the magnitude of change is variable. Of the single CK receptor mutants, *ahk2-1* and *ahk2-5* are sensitive to TCSA, while *ahk3-1* and *cre1-2* (*ahk4*) are resistant, suggesting that reduced regeneration by TCSA involves AHK3 and AHK4 (Figures 3A,C,D,H,I,M,N). Consistently, *ahk2-5 ahk3-7*, *ahk2-2 ahk3-3*, *ahk3-7 cre1-2* and the triple mutant are TCSA-resistant as well. Stronger TCSA responsiveness in *ahk2-5 cre1-2* compared to *ahk2-5 ahk3-7* or *ahk2-2 ahk3-3* implies that AHK3 is most susceptible to inhibition, although AHK4 was previously reported to be the most important CK receptor for *de novo* organogenesis in roots (Pernisova et al., 2018). Accordingly, regeneration is compromised in untreated *cre1-2* and higher order *ahk* mutants (Figures 3A,D), highlighting the importance of AHK4 (combined with AHK2 and AHK3) for



shoot regeneration. Overall, genetic loss of *AHK* function shows interplay with chemical inhibition.

Single mutants in phosphotransfer proteins acting downstream of AHKs in CK perception show similar regeneration levels and TCSA responsivity to WT Col-0

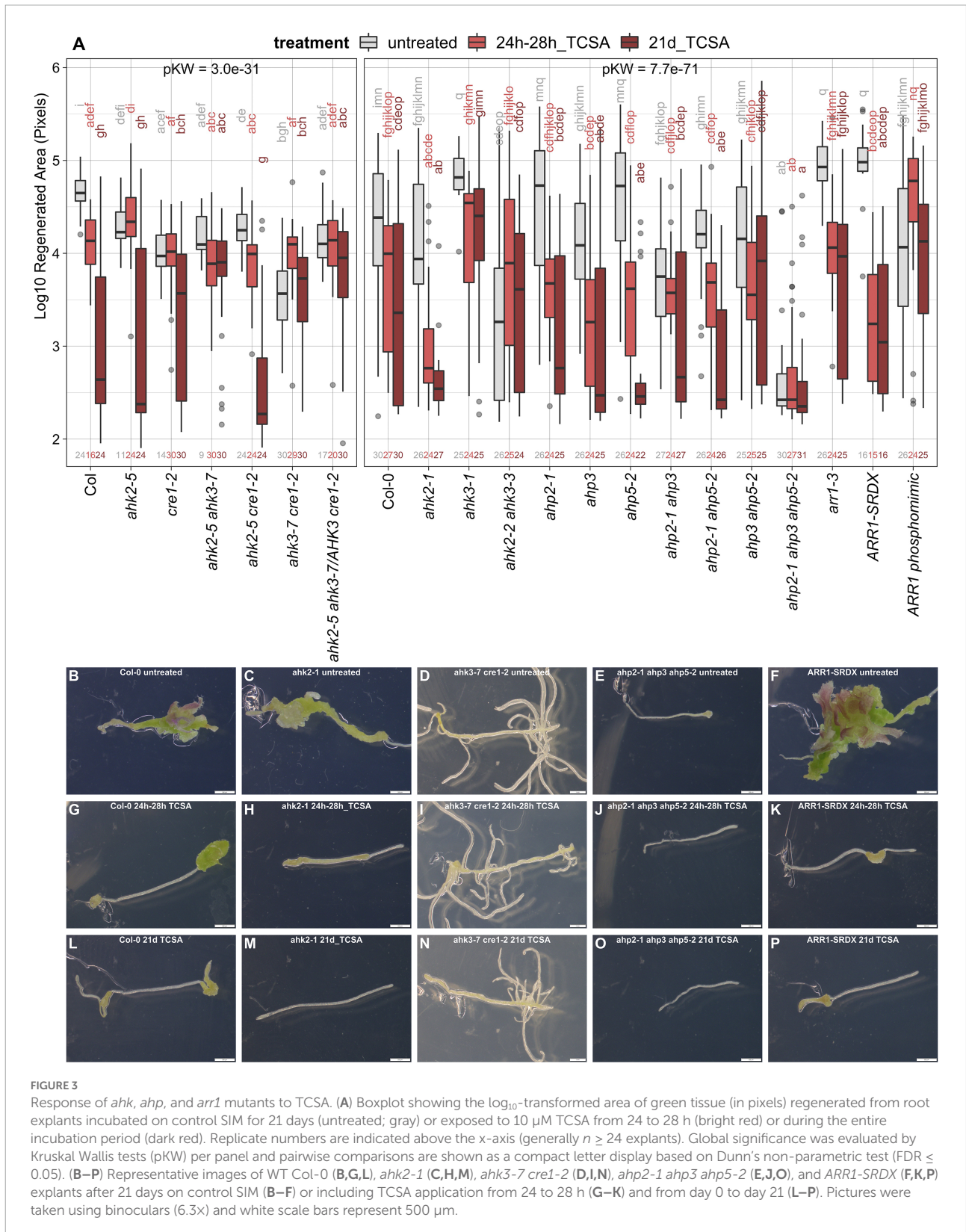
(Figure 3A), indicating functional redundancy among the AHPs. Whereas *ahp2-1 ahp5-2* and to a lesser extent *ahp2-1 ahp3* remain sensitive to TCSA, *ahp3 ahp5-2* and especially *ahp2-1 ahp3 ahp5-2* are TCSA-resistant. This suggests that AHP3 and AHP5 are susceptible to TCSA. Besides, control regeneration is



reduced in *ahp2-1 ahp3* and the triple mutant fails to regenerate under all conditions (Figures 3A,E,J,O). Therefore, multiple loss of AHP function phenocopies TCSA treatment, suggesting that AHPs are also involved in TCSA-reduced regeneration. Further downstream of the AHK-AHP signaling cascade, B-type response regulators such as ARR1 activate transcriptional CK responses. ARR1 directly binds the promoter of the shoot stem cell regulator *WUS* (Meng et al., 2017; Zhang et al., 2017), but indirectly represses *CLV3* and *WUS* via competition with ARR12 and induction of the auxin signaling repressor *INDOLE-3-ACETIC ACID INDUCIBLE 17* (*IAA17*; Liu et al., 2020). In agreement with an inhibitory role for ARR1 in shoot development, regeneration is increased in *arr1-3* mutants and explants containing the dominant *ARR1-SRDX* repressor (Figures 3A,F). Congruently, a constitutively active ARR1 phosphomimic (*35S::ARR1<sup>D94E</sup>*) reduces organogenic competence. Sensitivity of *arr1* loss-of-function mutants to TCSA (Figures 3A,F,K,P) implies that ARR1 is not a direct target and corroborates the involvement of upstream signaling modules. Additionally, gain-of-function mutants show reduced control regeneration and TCSA responsiveness, which suggests that blocking CK perception has no additional effect over excessive ARR1 activity or vice versa. Taken together, these data confirm

that canonical cytokinin signaling is required for shoot formation on SIM and suggest that TCSA inhibits regeneration through inhibition of this pathway.

To elucidate the impact of TCSA on hormone responses during shoot regeneration, we analyzed reporter lines for auxin (*proDR5::GFP*) and cytokinin activity (*proTCSn::GFP*) before and after TCSA or mock treatment from 24 to 28 h on SIM. For comparison, we also assessed transcriptional dynamics of the shoot markers *WUS* and *SHOOT MERISTEMLESS* (*STM*) via *proWUS::tdTom* and *proSTM::GFP*. Because AHK4 is the most important CK receptor for root-to-shoot conversion (Pernisova et al., 2018) and *cre1-2* (*ahk4*) mutants showed differential TCSA responses (Figure 3A), we analyzed *proTCSn::GFP* and *proWUS::tdTom* reporters in WT and *ahk4*. While *proTCSn::GFP* activity in WT steadily increases in the first 5 days upon transfer to cytokinin-rich SIM, it does not reach the same levels in mock-treated *ahk4* explants, confirming the importance of AHK4 for CK perception in the root. Surprisingly, TCSA has limited impact on *proTCSn::GFP* intensity in WT and only represses CK responses in the *ahk4* mutant from day three to day five on SIM (Figures 4A,B,G-L), which suggests that residual CK signals, transmitted by



TCSA-resistant AHKs during SIM incubation, are sufficient to trigger the sensitive *proTCSn::GFP* reporter. Similarly, *proWUS::tdTom* intensity in WT rises after 3 days on SIM and

this induction is delayed by TCSA application (Figures 4C,M,O,Q). In *ahk4*, *WUS* transcription is also induced from day three to day five, but it only reaches about

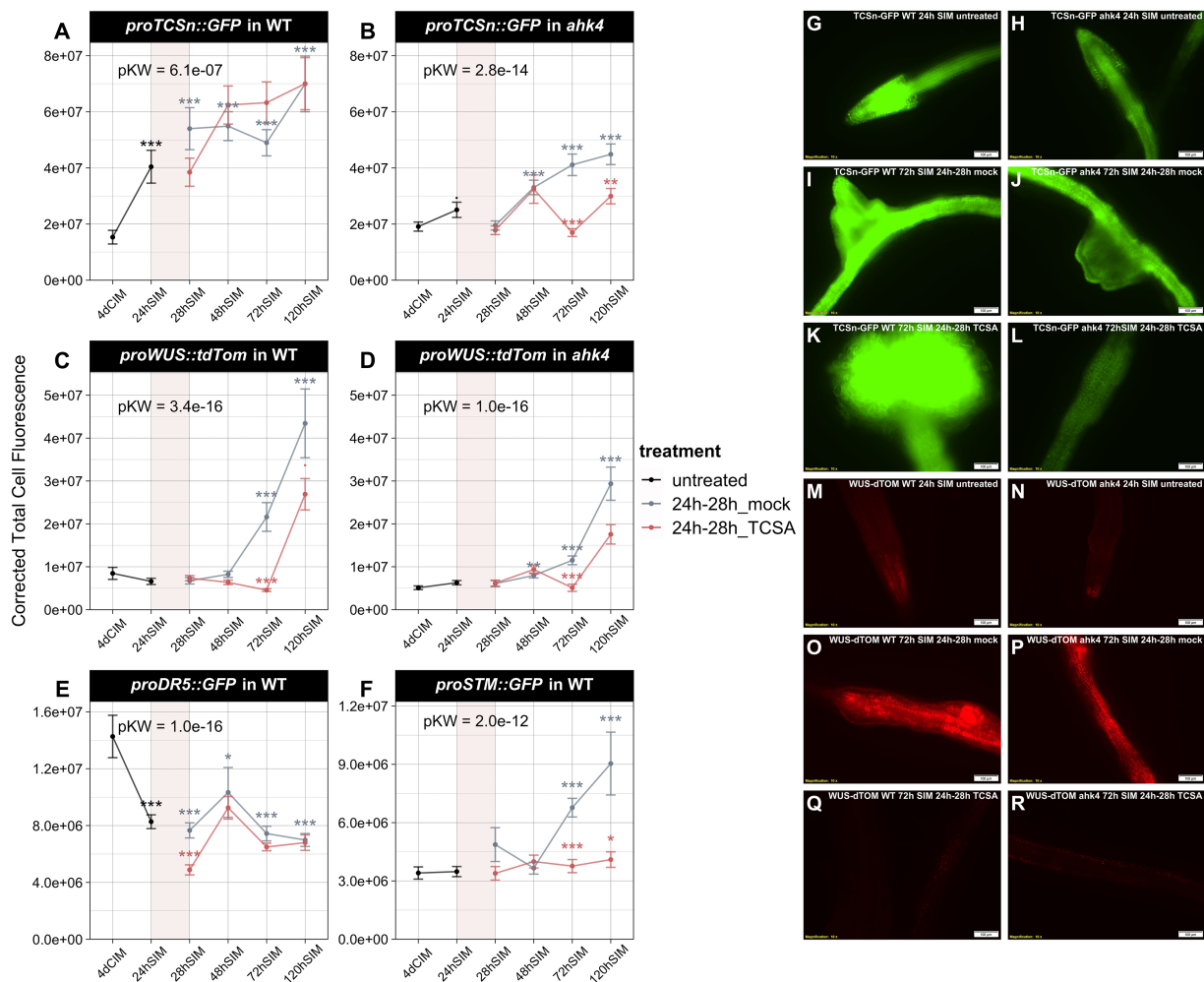


**FIGURE 4**  
 Analysis of TCSn, DR5, WUS, and STM reporters in wild type (WT) and *ahk4* mutants before and after TCSA or mock treatment. (A,B) *proTCSn::GFP* fluorescence in WT and *ahk4*. (C,D) *ProWUS::tdTom* fluorescence in WT and *ahk4*. (E,F) *ProDR5::GFP* and *proSTM::GFP* fluorescence in WT. Line plots show corrected total cell fluorescence (see Materials and methods) in root explants at several time points before and after treatment with 10  $\mu$ M TCSA or mock from 24 to 28 h on SIM (represented as a transparent red block in each graph). Global significance was determined by Kruskal Wallis tests per panel (pKW) and asterisks reflect FDR-adjusted *p*-values for pairwise Wilcoxon's tests comparing TCSA treatment to corresponding mock samples and mock treatment to untreated samples after 4 days on CIM ( $\cdot = p < 0.1$ ,  $\ast = p < 0.05$ ,  $\ast\ast = p < 0.01$  and  $\ast\ast\ast = p < 0.001$ ). (G–L) Representative images of *proTCSn::GFP* fluorescence in WT (G,I,K) and *ahk4* (H,J,L) after 24 h (G,H) and 72 h on SIM with mock (I,J) or TCSA treatment (K,L) between 24 and 28 h. (M–R) Representative images of *proWUS::tdTom* fluorescence in WT (M,O,Q) and *ahk4* (N,P,R) after 24 h (M,N) and 72 h on SIM with mock (O,P) or TCSA treatment (Q,R) between 24 and 28 h. Pictures were taken using a fluorescence microscope (10 $\times$ ).

70% of WT expression in the mock condition and the response is even lower after administering TCSA (Figures 4D,N,P,R). Despite the limited *proTCSn::GFP* activity in this context, there is a slight surge in *WUS* levels in TCSA-treated *ahk4* roots, indicating residual CK responses or activation of *WUS* transcription by other pathways. The *proDR5::GFP* marker is rapidly repressed after transfer to SIM in both mock and TCSA-treated root segments (Figure 4E), which shows that auxin is not a primary determinant of TCSA-impaired shoot regeneration. On the other hand, *proSTM::GFP* intensity strongly increases after 2 days on SIM in the mock condition, but this effect is not observed after exposure to TCSA (Figure 4F). Hence, STM is a downstream

target of TCSA, acting in parallel of reduced AHK signaling and delayed *WUS* expression. Deregulation of shoot markers by TCSA contradicts the weak perturbation of transcriptional hormone responses, so TCSA likely affects other processes that converge with CK signaling during regeneration.

## Phosphoproteome analysis uncovers TCSA-responsive phosphosites

Because TCSA is a putative kinase inhibitor and mutant analyses hint at multiple targets including CK signaling components and shoot meristem markers, a phosphoproteome analysis was

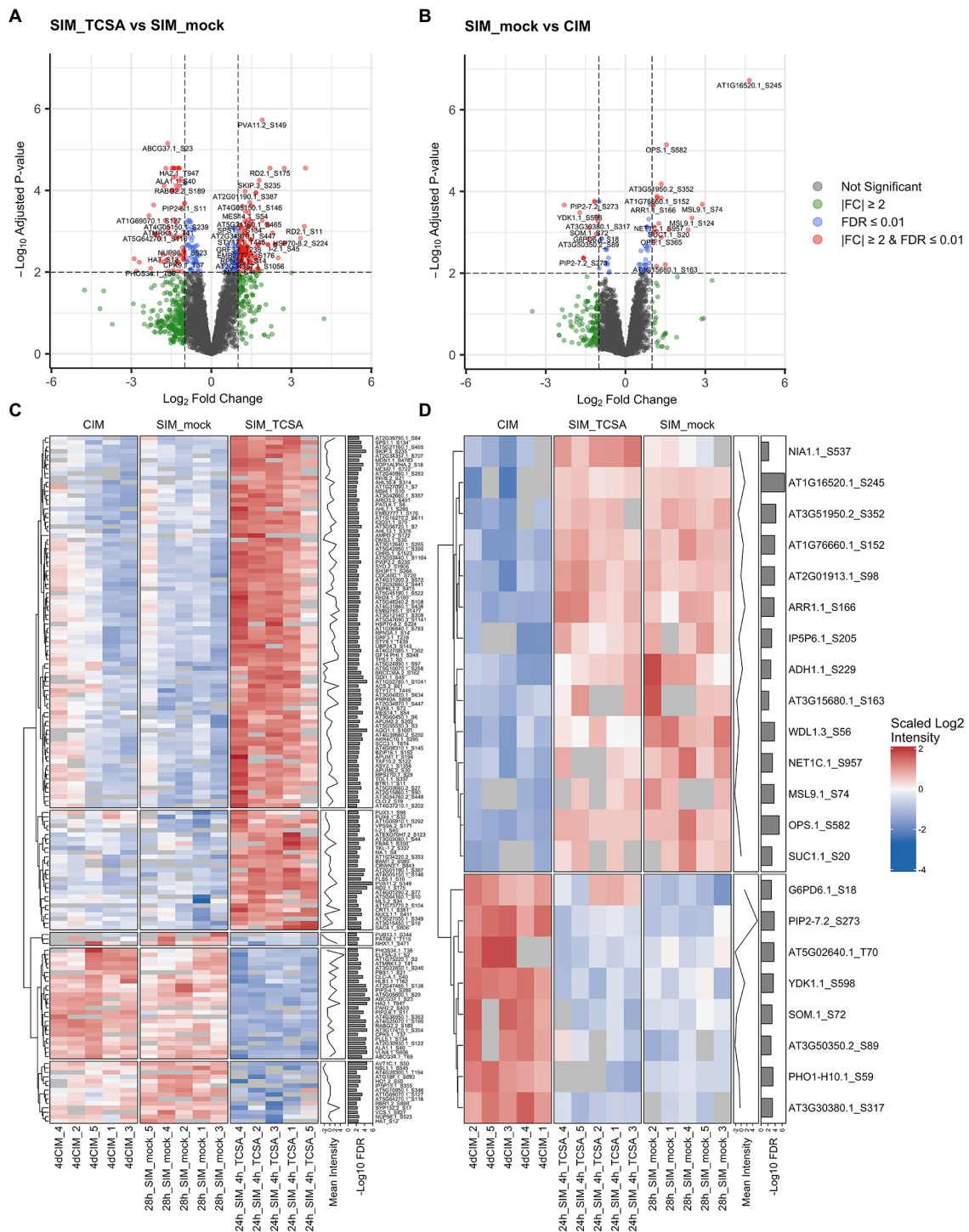


**FIGURE 5** Phosphoproteome analysis of root explants on CIM and SIM following TCSA or mock treatment. **(A,B)** Volcano plots comparing phosphosite intensities after 28 h on SIM with 10  $\mu$ M TCSA or mock treatment in the last 4 h (SIM\_TCSA vs. SIM\_mock), and after 28 h on control SIM or 4 days on CIM (SIM\_mock vs. CIM). Gray dots represent non-significant values, green dots reflect absolute fold changes (FC) above 2, blue dots show phosphosites with an FDR below 0.01, and red dots indicate significant phosphosites (at  $FDR \leq 0.01$ ) with  $|FC| \geq 2$ . **(C,D)** Heatmaps of scaled  $\log_2$  intensities for top DRPs between root explants treated with TCSA or mock from 24 to 28 h on SIM (24h\_SIM\_4h\_TCSA vs. 28h\_SIM\_mock; red dots in panel **A**), and after 24 h on SIM or after 4 days on CIM (28h\_SIM\_mock vs. 4dCIM; red dots in panel **B**). Clustering is based on Euclidean distances and annotation columns show mean  $\log_2$  intensities (before scaling) and  $-\log_{10} FDR$  values per row. In case of redundancy only the most significant phosphosite per gene was retained.

conducted to uncover phosphorylation dynamics underlying TCSA-responsive shoot regeneration. To prioritize events parallel and downstream of CK perception, we focused on Ser/Thr/Tyr rather than His phosphoproteins and selected a long application window in terms of PTMs (4h). Specifically, the phosphoproteome of root tissues was evaluated after TCSA or mock treatment from 24 to 28 h on SIM. As an additional control, we collected samples just before transfer to SIM. Total protein content was extracted, digested, and enriched for O-phosphopeptides prior to liquid chromatography (LC)-MS/MS analysis. Peptide identification and quantification were done in MaxQuant and the DEqMS package (based on limma) was used for statistical testing (Cox and Mann, 2008; Ritchie et al., 2015; Tyanova et al., 2016a; Zhu et al., 2020b). Comparing TCSA and mock-treated roots reveals 324 differentially regulated phosphosites (DRPs) at an FDR of 0.01, of which 202 are upregulated and 122 are downregulated upon TCSA treatment (Table 1; Figure 5A; Supplementary Data 1). The intensity of 205 of these DRPs increased or decreased at least two-fold (either implying that the site undergoes phosphorylation changes or that the (phospho) peptide abundance varied). The majority of DRPs concern S residues, while 40 are T residues. Of the 243 unique proteins identified, respectively 190, 37, 9, and 6 proteins harbor one, two, three or four DRPs. Additionally, the amino acid transporter AVT1C contains seven deregulated serine residues, six of which exhibit strong negative fold changes (Table 1). A heatmap of phosphosites (one per gene) with FDRs below 0.01 and absolute  $\log_2$  fold changes (LFCs) above 1 highlights the discrepancy between CIM and control SIM on one hand and TCSA treatment on the other hand (Figure 5C). Hierarchical clustering roughly distinguishes five clusters, the two largest of which contain DRPs with low to moderate intensities on control SIM or CIM that are upregulated by TCSA, while three smaller clusters show moderate to high values for mock or CIM and downregulation after TCSA treatment. Intriguingly, many sites show opposite behavior when comparing CIM to mock or TCSA samples, suggesting that TCSA reverses phosphorylation trends required for regeneration. Based on statistical significance and fold changes, the most interesting candidate genes are *AGO1*, *RD2*, *AT1G52780*, *PVA11*, and *AVT1C* ( $FDR \leq 10^{-4}$  and  $|LFC| \geq 2$ ). Other highly significant sites are located in *ABCG37*, *PIP2;4/PIP2F*, *NSL1*, *CARK1*, *HA2*, and *VLN4* (Table 1). Three and 12 phosphosites are, respectively detected in TCSA or mock-treated samples only (Supplementary Table 1; Supplementary Data 1).

Notably, 4 h of TCSA treatment has a stronger impact on phosphoproteome dynamics than 24 h incubation on cytokinin-rich SIM, as only 78 phosphosites are differentially regulated on control SIM versus CIM at  $FDR \leq 0.01$  (Table 1; Supplementary Data 1). Respectively 50 and 28 of these show increased and reduced levels on SIM, with 32 undergoing at least two-fold intensity changes (Figure 5B). These DRPs correspond to 58 unique proteins, 12 of which contain two or three phosphosites (and two of the three downregulated sites in the aquaporin *PIP2;7/PIP3A* can carry one or two phosphate groups). Respectively 68, 9, and 1 of the positions involve S, T, and Y residues. For DRPs with FDRs below 0.01 and LFCs

above 1, a heatmap reveals similar trends on SIM with mock or TCSA treatment compared to CIM samples, and two clusters can be discerned (Figure 5D). The largest is made up of DRPs with increased phospholevels on SIM versus CIM, while the smaller one shows opposite behavior. Intriguingly, *NAIP2.1* shows 25-fold higher intensity of phosphorylated S245 after 24 h on SIM and is required for the biogenesis of ER-derived vesicles (Wang et al., 2019b). Other top phosphosites are in *OPS* and *AT3G51950* ( $FDR \leq 10^{-4}$ ), *MSL9* and *AT5G02640* ( $|LFC| \geq 2$ ). Notable prior candidates are *ARR1* (containing three upregulated S residues at positions 166, 168, and 190), *QKY*, and *BAM1* (both harboring one upregulated serine). Although the affected serines in *ARR1* are not implicated in the canonical His-Asp CK signaling phosphorelay, differential regulation of *ARR1* on SIM vs. CIM but not TCSA vs. mock supports a role in shoot regeneration based on mutant analyses (Figures 3A,F,K,P) and confirms that it is not a direct TCSA target. Furthermore, 4 out of 13 plasma membrane (PM) integral proteins (PIPs) in *Arabidopsis* undergo reduced S/T phosphorylation on SIM (*PIP2;7*, *PIP2;2*, *PIP2;6*, and *PIP2;4*). *PIP2;6* and *PIP2;4* have an  $FDR \leq 0.01$  in both comparisons (TCSA vs. mock or control SIM vs. CIM treatment), along with *BAM1*, *NIA1*, *EDR2*, and *AT4G38550*. Finally, five phosphosites are found only after CIM incubation and two phosphosites are unique for mock SIM (Supplementary Table 1; Supplementary Data 1).

## Enriched functionalities among deregulated phosphoproteins

To obtain more insight into the molecular pathways and processes affected by TCSA, a gene set enrichment analysis (GSEA) was performed on all 522 genes that harbor significantly deregulated phosphosites between TCSA and mock treatment (at  $FDR \leq 0.05$ ). The results are presented in a functional network produced by the ClueGO plugin for Cytoscape (Shannon et al., 2003; Bindea et al., 2009, 2013), showing 75 enriched terms (alongside 174 input genes mapping to these terms), organized into 16 groups and connected based on gene overlap (Figure 6; Supplementary Figure 2). Overview terms per group were selected by significance. The most important clusters relate to protein modification (bright red; 11 terms and 38 genes), mRNA splicing (purple; 6 terms and 38 genes), Golgi vesicle transport (dark red; 9 terms and 22 genes), plant organ morphogenesis (bright green; 10 terms and 34 genes), cation transmembrane transport or gluconeogenesis (bright blue; 20 terms and 31 genes), and meristem growth (light green; 5 terms and 17 genes). The occurrence of terms such as meristem maintenance, embryonic meristem development, shoot system morphogenesis, leaf development, root morphogenesis, root epidermal cell differentiation, etc. corroborates that TCSA interferes with multiple (phospho) proteins related to *de novo* organogenesis. The top deregulated proteins ( $FDR \leq 10^{-3}$  and  $|LFC| \geq 1$ ) in this group

TABLE 1 Deregulated proteins containing at least one highly significant phosphosite ( $FDR \leq 10^{-4}$ ) when comparing TCSA to mock SIM and/or mock SIM to CIM treatment (Supplementary Data 1).

Contrast	Protein	Site	$P_i$	LFC	Mean	FDR	Gene ID	Description
TCSA vs. mock	PVA11.2	S149	1	1.91	2.75	1.89E-06	AT3G60600	Vesicle-associated protein 1-1
		S2	1	-1.92	-2.34	1.48E-03		
	ABCG37.1	S23	1	-1.64	-0.50	7.02E-06	AT3G53480	ABC transporter G family member 37
	AGO1.1	S1001	1	3.53	-0.94	2.84E-05	AT1G48410	Protein argonaute 1
	AT1G52780.1	S1041	1	2.73	-2.15	2.84E-05	AT1G52780	PII, uridylyltransferase (DUF2921)
			1	2.20	-0.33	2.84E-05	AT2G21620	
	RD2.1	S175	1	3.49	-1.51	7.60E-04	AT2G39130	Amino acid transporter AVT1C
			1	-1.71	-1.49	2.84E-05		
			2	-1.41	0.95	2.84E-05		
			2	-1.41	0.95	2.84E-05		
			1	-1.48	-1.10	9.81E-05		
			2	-2.16	-0.85	2.26E-04		
			1	-1.03	-0.26	1.23E-03		
			1	1.04	0.57	2.31E-03		
			1	-1.20	0.90	3.83E-03		
			1	-0.70	-0.46	9.57E-03		
	NSL1.1	S545	1	-1.41	-2.52	2.84E-05	AT1G28380	MACPF domain-containing protein NSL1
	CARK1.1	S354	2	-1.27	1.59	2.84E-05	AT3G17410	Receptor-like cytoplasmic kinase 1
			2	-1.27	1.59	2.84E-05		
	HA2.1	T947	1	-1.20	3.88	2.84E-05	AT4G30190	ATPase 2, plasma membrane-type
			1	-1.29	0.90	1.48E-03		
	VLN4.1	S806	1	-1.19	2.18	2.84E-05	AT4G30160	Villin-4
			1	-0.84	3.31	1.39E-03		
	ALA1.1	S40	1	-1.33	1.36	4.47E-05	AT5G04930	Phospholipid-transporting ATPase 1
			1	-0.77	0.64	6.00E-04		
			1	-1.03	0.21	4.76E-03		
	PLL5.1	S134	1	-1.44	-0.76	4.80E-05	AT1G07630	Probable protein phosphatase 2C 4
1			-1.27	-1.67	9.71E-05			
SKIP3	S235	1	1.79	-0.88	5.66E-05	AT1G77180	SNW/SKI-interacting protein	
		2	0.94	4.41	3.13E-03			
		2	0.94	4.41	3.13E-03			
AT1G77180.1	S190	1	-1.13	0.77	5.66E-05	AT1G77180	Caldesmon-like protein	
		1	-1.32	-1.06	7.72E-05			
		1	-1.48	-0.33	9.98E-05			
AT2G47485.1	S138	1	-1.21	0.25	5.73E-05	AT2G47485	Hypothetical protein	

(Continued)

TABLE 1 Continued

Contrast	Protein	Site	P <sub>i</sub>	LFC	Mean	FDR	Gene ID	Description
TCSA vs. mock (mock vs. CIM)	AT1G56140.1	S1003	1	-0.99	-1.22	6.67E-05	AT1G56140	LRR receptor-like Ser/Thr-protein kinase
	CASP1	S589	1	-0.97	1.69	6.67E-05	AT3G18480	Protein CASP
	AT2G30930.1	S122	1	-1.77	-0.02	7.72E-05	AT2G30930	Expressed protein
	RABG2.2	S189	1	-1.19	-0.75	7.72E-05	AT2G21880	Ras-related protein RABG2
	JOX2.1	S29	1	-1.44	0.84	9.98E-05	AT5G05600	Jasmonate-induced oxygenase 2
	PIP2-4.1	S286	1	-1.48	2.63	2.84E-05	AT5G60660	Probable aquaporin PIP2-4
Mock vs. CIM	NAIP2.1	S245	1	4.66	1.30	1.90E-07	AT1G16520	NAI1 interacting protein
	OPS.1	S582	1	1.54	-0.99	7.19E-06	AT3G09070	Protein OCTOPUS
		S241	1	1.17	-1.29	9.35E-04		
TCSA vs. mock (mock vs. CIM)		S365	1	1.35	-1.53	1.32E-03		
	AT3G51950.2	S352	1	1.35	-1.09	6.54E-05	AT3G51950	Zinc finger CCCH domain protein 46

are VLN4, AGO1, PLL5, TOP1ALPHA, and MCM2, while other interesting members with respect to literature are BAM1, PIN1, EIN2, BIN2, TPR2, JKD, RBR1, and FIP37.

Enrichment of terms like cellular response to organic cyclic compound, regulation of protein modification process, and regulation of phosphate metabolic process further shows that TCSA influences post-translational control mechanisms. This involves I-2, GF14 PHI, PC-MYB1, ELF5A-3, DMS3, and SNF4. Less anticipated pathways include exocytosis, vesicle docking, and auxin polar transport (e.g., ABCG37, CASP, SYP132, and GSO11), inorganic ion transmembrane transport (e.g., HA2, CLC-A, and NHX1), RNA splicing, mRNA processing, and post-transcriptional gene silencing (e.g., AGO1, SKIP, PRP40A, PWP2, and AT2G34970). These imply extensive cellular deregulation by TCSA treatment. Moreover, carbon assimilation and energy metabolism are also affected. Noteworthy smaller groups are those involving defense responses, cytokinesis, histone deacetylation, and autophagy. When less stringent enrichment filters are applied, additional terms emerge (Supplementary Figure 2), such as signal transduction by protein phosphorylation (e.g., ATMAP4K ALPHA1, MAP3KA, MEKK1, SIK1), brassinosteroid-mediated signaling pathway (e.g., BIN2, BSK5, BSL1, BSL3, GF14 PHI), and cellular response to heat (e.g., BAG7, HSBP, LARP1a). Central hubs in the network are RS40&41, TGH, HA1-3, AGO1, VCS, and DDL (degree  $\geq 10$ ), while SYP122, MPK4, AGO1, NHX1, PAPS1, KT1, VCS, PCK1, and CRT1a form important connections between distant hubs (betweenness  $\geq 3,000$ ).

## Discussion

Consistent with the reported inhibition of cytokinin signaling by salicylanilides in periwinkle cells (Papon et al., 2003), TCSA impedes shoot regeneration from roots in *Arabidopsis thaliana*, which is most effective for short applications in the first 4 days of SIM incubation. The fold change of the effect was largest in Ws, while the absolute difference correlated with the regenerative potential of tested accessions. Mutant analyses showed that TCSA interferes directly or indirectly with AHKs and AHPs, of which AHK3, AHK4, AHP3, and AHP5 are prime candidates. Further biochemical evidence is needed to assess whether these interactions are direct. Inhibition of His autokinase activity by salicylanilides in bacterial two-component systems occurs *via* structural alteration and aggregation of the catalytic domain, supporting the notion that both AHKs and AHPs could be directly affected by TCSA, because both harbor a conserved His kinase domain (Stephenson et al., 2000). Although other HKs such as CKI1 and ETR1 have been linked to *de novo* organogenesis (Kakimoto, 1996; Chatfield and Raizada, 2008), it is unlikely that these are critical for inhibition of shoot regeneration by TCSA based on the genetic data and limited perturbation of TCSn activity by TCSA in WT. Repressing ARR1 functionality enhanced regeneration, whereas increased ARR1 activity reduced regeneration and TCSA susceptibility. Although ARR1 is a

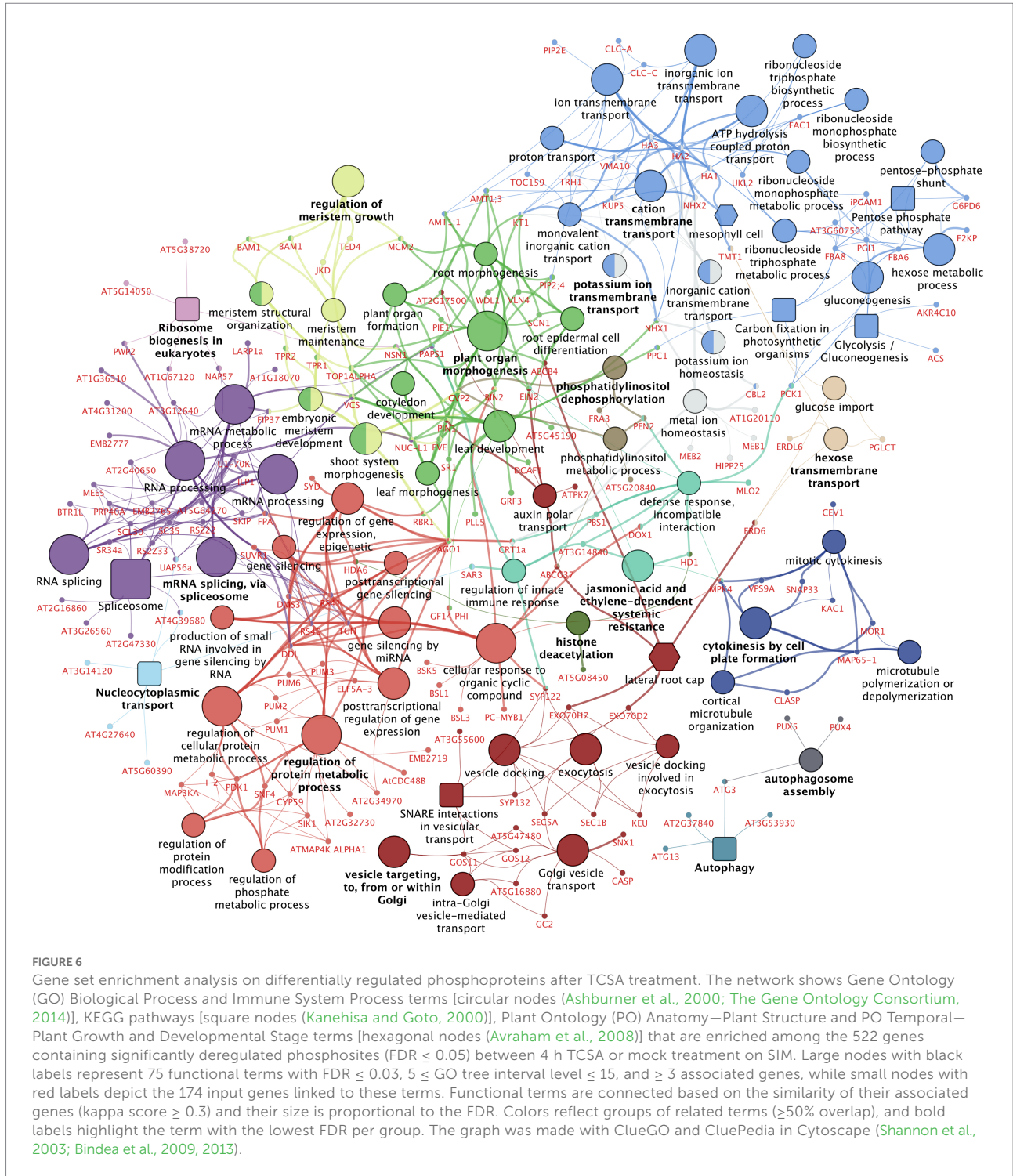


**FIGURE 6**  
 Gene set enrichment analysis on differentially regulated phosphoproteins after TCSA treatment. The network shows Gene Ontology (GO) Biological Process and Immune System Process terms [circular nodes (Ashburner et al., 2000; The Gene Ontology Consortium, 2014)], KEGG pathways [square nodes (Kanehisa and Goto, 2000)], Plant Ontology (PO) Anatomy—Plant Structure and PO Temporal—Plant Growth and Developmental Stage terms [hexagonal nodes (Avraham et al., 2008)] that are enriched among the 522 genes containing significantly deregulated phosphosites (FDR  $\leq$  0.05) between 4 h TCSA or mock treatment on SIM. Large nodes with black labels represent 75 functional terms with FDR  $\leq$  0.03, 5  $\leq$  GO tree interval level  $\leq$  15, and  $\geq$  3 associated genes, while small nodes with red labels depict the 174 input genes linked to these terms. Functional terms are connected based on the similarity of their associated genes (kappa score  $\geq$  0.3) and their size is proportional to the FDR. Colors reflect groups of related terms ( $\geq$ 50% overlap), and bold labels highlight the term with the lowest FDR per group. The graph was made with ClueGO and CluePedia in Cytoscape (Shannon et al., 2003; Bindea et al., 2009, 2013).

transcriptional activator in the CK signaling pathway (Sakai et al., 2000), it inhibits shoot regeneration through competition with ARR12 (Meng et al., 2017; Zhang et al., 2017; Liu et al., 2020). Because the latter induces *WUS*, an imbalance in active B-type ARR levels caused by TCSA might explain the observed effects. Notably, our phosphoproteome data also reveal deregulation of ARR1 S-phosphoproteins on SIM vs. CIM, but not in response to TCSA. Although serine phosphorylation of ARR1 has not been

reported, CK prevents proteasomal degradation of this TF and serine phosphorylation of A-type ARRs enhances their stability (Kurepa et al., 2014b; Huang et al., 2018). As we find three upregulated phosphoserines in ARR1.1 upon CK treatment (S166, S168, and S190), it is possible that CK exploits similar mechanisms to mediate the activity of B-type ARRs. Reporter lines further reveal that TCSA application delays *WUS* expression and impairs *STM* induction on SIM, which is at least partly independent of CK

signaling. Although Closantel<sup>®</sup> was reported to have similar specificity as TCSA (Papon et al., 2003), shoot regeneration from root explants is resistant to this inhibitor. This agrees with the lower potency of Closantel<sup>®</sup> in periwinkle and suggests that it might be degraded after prolonged exposure to light, metabolized, or poorly absorbed in *Arabidopsis* root cells. Additionally, our results show that rapamycin can enhance *de novo* shoot organogenesis, indicating that AtFKBP12 is not completely insensitive to the compound. This was also observed in cell suspension cultures, where many phosphopeptides underwent similar changes after treatment with rapamycin or the more potent TOR inhibitor AZD8055 (Van Leene et al., 2019), and under anaerobic conditions that partially restore AtFKBP12 functionality to retard growth in the presence of rapamycin (Deng et al., 2016). Accordingly, inconsistent rapamycin resistance in *Arabidopsis* has been attributed to variable endogenous FKBP12 content (Xiong and Sheen, 2012). As TOR is required for auxin responses, rapamycin could enhance shoot formation on SIM by tilting the balance of auxin-cytokinin antagonism in favor of CK signals.

A phosphoproteome analysis shows that besides inhibition of His phosphorylation, TCSA also has a strong impact on phosphorylation of Ser, Thr and Tyr, because 324 O-phosphosites are significantly deregulated after 4h of TCSA treatment (at  $FDR \leq 0.01$ ; Supplementary Data 1). By contrast, only 78 DRPs are found when comparing explants kept on control SIM for 24h vs. CIM. PIP2;4, PIP2;6, AT4G38550, BAM1, NIA1, and EDR2 contain DRPs that respond to both treatments, but only half of the targeted residues are conserved and all show similar trends when comparing TCSA and mock or SIM and CIM. Hence, the link with disrupted cytokinin signaling is difficult to assess. Černý et al. previously showed that many early cytokinin response phosphopeptides relate to protein regulation and gene expression (Cerny et al., 2011), which are also enriched ontologies in our data. Despite detecting only 29 phosphoproteins, they reported increased levels of phosphorylated COR47, which is downregulated by TCSA. A comparison of Ser/Thr/Tyr phosphorylation in WT and *ahk2 ahk3* mutants (with or without cytokinin) further identified nine proteins that also exhibit differential phospholevels after mock or TCSA treatment (e.g., PIP2;4, NET1C, and CDC48D), although most show conflicting trends (Dautel et al., 2016). Still, the number of unique phosphoproteins that respond to TCSA (243) is similar to the number of differentially phosphorylated proteins during protoplast regeneration in *Physcomitrium patens* (i.e., 300), and substantial overlap exists among enriched annotations (e.g., transcriptional regulation, transport, metabolism, cell division, and morphogenesis; Wang et al., 2014b). On the other hand, only nine phosphoproteins were deregulated during dedifferentiation of cotyledon cells in *Arabidopsis*, but this is likely due to the poor resolution and sensitivity of 2-DE gel assays (Chitteti and Peng, 2007). Although the latter study detected several 14–3–3-like proteins and such factors also appear in our phosphoproteome, none of the phosphosites overlap with our DRPs. Surprisingly, the majority of TCSA-responsive phosphosites exhibit increased intensities, despite its putative role as a His kinase inhibitor (Papon et al., 2003; Desikan

et al., 2008). It is possible that these observations reflect indirect effects because sampling was done after 4h and our analysis focused on Ser/Thr/Tyr residues. If and how elevated Ser/Thr/Tyr phospholevels contribute to impaired shoot regeneration depends on the role of deregulated phosphoproteins in organogenesis and the effect of phosphorylation on their activity. Interpretation of the results is further complicated because we cannot distinguish between differential phosphorylation or peptide abundance.

Twenty-four phosphopeptides are unique for a specific treatment group (Supplementary Table 1; Supplementary Data 1), but they are not linked to obvious candidates and could reflect negligible differences. Based on statistical significance, top TCSA targets are *AGO1*, *RD2*, *AT1G52780*, *PVA11*, and *AVT1C* (Table 1; Supplementary Data 1). ARGONAUTE (AGO) proteins mediate (post)transcriptional gene regulation through association with microRNAs (miRNAs) to form RNA-induced silencing complexes (RISC; Wilson and Doudna, 2013). We find that the serine residue at position 1,001 in AGO1.1 is more than 11-fold upregulated upon TCSA treatment. This phosphosite is also deregulated by H<sub>2</sub>O<sub>2</sub> and was suggested to affect silencing activity because it is just downstream of the PIWI domain (Bentem et al., 2008). AGO1 is involved in various aspects of plant development and mutants show pleiotropic phenotypes (Kidner and Martienssen, 2005; Zhang and Zhang, 2012). Together with its close homolog AGO10/ZLL/PNH, AGO1 controls stem cell maintenance in the SAM by fine-tuning the activity of miR165/166, which target HD-ZIP III TFs (e.g., *PHB*, *PHV*, and *REV*) that interact with B-type ARRs to potentiate *WUS* expression (Zhang et al., 2017; Chang et al., 2020). While *AGO1* is ubiquitously expressed and promotes degradation of *HD-ZIP III* transcripts via miR165/166, AGO10 is confined to the SAM and the adaxial side of organ primordia to protect HD-ZIP III TFs by sequestering miR165/166 (Liu et al., 2009; Zhu et al., 2011; Zhang and Zhang, 2012; Zhou et al., 2015). Suppression of HD-ZIP III TFs by AGO1 further depends on miR168-directed autorepression and availability of SQN and HSP90 chaperones (Du et al., 2020). Notably, AGO1 was previously suggested to modulate *STM* levels (possibly involving *CUC1-2* targeting by miR164), and HD-ZIP III TFs can activate *STM* as well (Laufs et al., 2004; Kidner and Martienssen, 2005; Shi et al., 2016). Enhanced AGO1 function by phosphorylation might thus hamper shoot formation by repressing *HD-ZIP III* and downstream *WUS* (and/or *STM*) independent of CK (Zhang and Zhang, 2012; Chang et al., 2020). However, conflicting roles have been reported for the AGO10—miR165/166—HD-ZIP III module during *in vitro* shoot regeneration (Xue et al., 2017; Lardon and Geelen, 2020).

Phospholevels are also increased by TCSA at two positions in RD2.1, with over 11-fold changes for S11 and over four-fold changes for S175. RD2 is involved in dehydration and desiccation responses, but it has not been associated with organogenesis before. Next, *AT1G52780* encodes a poorly characterized PII-uridylyltransferase (DUF2921) associated with the trans-Golgi network and S1041 in *AT1G52780.1* shows more than six-fold higher intensity after exposure to TCSA (Groen et al., 2014). Uridylylation of PII signal transduction proteins mediates carbon

and nitrogen sensing in the chloroplasts, but the link with regeneration is unclear (Hsieh et al., 1998; Chen et al., 2006). Vesicle-associated protein 1–1 (PVA11/VAP27-1) is required for endocytosis and autophagy through interaction with NET3C, the cytoskeleton, phosphatidylinositol-phosphate lipids, and clathrin at contact sites between the endoplasmic reticulum (ER) and the PM (Wang et al., 2014a, 2019a; Stefano et al., 2018). Misexpression causes pleiotropic defects, including aberrant root development (Wang et al., 2016). Phosphorylation is over three-fold increased or decreased at S149 and S2 in PVA11.2, respectively. Although proper endocytic trafficking is a prerequisite for *de novo* organogenesis (Dhonukshe et al., 2007; Kitakura et al., 2011; Marhavý et al., 2011; Liu et al., 2018), the effect of phosphorylation on PVA11 activity is unknown. The AVT1C protein contains seven deregulated S residues, six of which are downregulated with fold changes from two to four (S50, S87, S92, S126, S127, and S132; note that S126 and S132 can carry single or double modifications), while S14 is upregulated over two-fold. Another phosphosite in AVT1C (S91) is only detected on control SIM and CIM (Supplementary Table 1). Although little is known about this vacuolar amino acid transporter, AVT1B was predicted to be downregulated in shoots by high nitrogen-induced ARR4 (Heerah et al., 2021).

Other highly significant DRPs in response to TCSA are located in ABCG37 (a pleiotropic auxin transporter that exports indole-3-butyric acid from the root apex (Růžička et al., 2010)), PIP2;4 (an aquaporin with a DRP at S286 that is also targeted by SIRK1 and phosphorylated under salt stress (Hsu et al., 2009; Wu et al., 2013)), NSL1 [a perforin restraining SA-induced defense responses (Noutoshi et al., 2006)], CARK1 [a kinase that enhances drought resistance by phosphorylating ABA receptors (Zhang et al., 2018)], HA2 [a PM H<sup>+</sup>-ATPase required to establish the proton motive force (PMF; Haruta and Sussman, 2012)], and VLN4 [an actin filament bundling protein involved in root hair growth (Zhang et al., 2011)]. Phosphorylation of T947 in HA2 hyperactivates the enzyme by creating a binding site for regulatory 14–3–3 proteins (Fuglsang et al., 1999, 2007; Kinoshita and Shimazaki, 1999). This site is downregulated by TCSA (while the 14–3–3 proteins GRF3 and GF14 PHI show increased phospholevels), suggesting that a reduced PMF might hamper regeneration, consistent with the finding that *aha2* mutants show defective root growth under physiological stresses and *aha1 aha2* is embryo lethal (Haruta et al., 2010). Besides, cytokinin-responsive ARR1 and auxin promote cell wall acidification and loosening *via* H<sup>+</sup>-ATPases to induce elongation and differentiation (Hager et al., 1991; Fendrych et al., 2016; Pacifici et al., 2018). Finally, QKY is a prior candidate containing DRPs between mock SIM and CIM. We previously found that this transmembrane protein underlies natural variation in shoot regeneration and loss-of-function enhances callus growth under specific conditions (Lardon et al., 2020). QKY also interacts with the LRR-RLK SUB to control plasmodesmata conductivity during organ morphogenesis and mutation causes aberrant SAM structures (Fulton et al., 2009; Trehin et al., 2013; Vaddepalli et al., 2014). Here, we show that QKY.1 exhibits increased phospholevels at S258 after 24 h on SIM versus CIM, confirming a role in organogenesis.

For 39 of the 522 genes (7.5%) affected by TCSA (at FDR ≤ 0.05), GSEA revealed a link with organ morphogenesis. The most interesting candidates in this category based on literature are *BAM1*, *FIP37*, *PIN1*, *RBR1*, *TOP1ALPHA*, *AGO1*, *BIN2*, *DCAF1*, *EIN2*, *JKD*, *MCM2*, *NSN1*, *PAPS1*, *PLL5*, and *TPR2*. *BAM1* and *PLL5* are involved in SAM patterning, as *BAM1* antagonizes *CLV1* and promotes *WUS* expression *via* ligand competition and *CLE40* signaling (DeYoung and Clark, 2008; Somssich et al., 2016; Schlegel et al., 2021). Although *PLL5* was only attributed a role in leaf development, it is a homolog of *POL*, acting downstream of *CLV1* in the repression of *WUS* by *CLV3* (Song and Clark, 2005; Song et al., 2006). Accordingly, *BAM1* and *PLL5* show contrasting phosphorylation trends in response to TCSA, but how this modulates their activity remains to be elucidated. *FIP37* controls shoot stem cell fate by confining the expression of *WUS* and *STM* through destabilizing N<sup>6</sup>-methyladenosine modification of mRNA, and loss-of-function causes SAM overproliferation (Shen et al., 2016). *TOP1ALPHA/FAS5* (Graf et al., 2010; Liu et al., 2014; Albert et al., 2015; Zhang et al., 2016), *RBR1* (Wildwater et al., 2005; Perilli et al., 2013; Ötvös et al., 2021), *NSN1* (Wang et al., 2011, 2012), *JKD* (Welch et al., 2007; Bustillo-Avenidaño et al., 2018), and *MCM2* (Ni et al., 2009; Huang et al., 2019a) also mediate meristem maintenance and organ patterning at the shoot or root apex, but none of the DRPs were previously reported. Next, *PIN1*, *PILS5*, *ABCB4*, and *ABCG37* play a role in (polar) auxin transport (Růžička et al., 2010; Barbez et al., 2012; Cho et al., 2012), which is pivotal to establish hormone gradients in organ primordia (Motte et al., 2014b; Lardon and Geelen, 2020). Phosphorylation by *PID/WAG*, *D6PK*, *PAX*, and *MAP* kinases controls directional auxin flow *via* activity modulation, polarity switches and re-localization of *PIN*s (Tan et al., 2021). For instance, S337 in the cytoplasmic loop of *PIN1* is phosphorylated by the *MKK7*—*MPK3/6* cascade, causing a basal-to-apical shift during shoot branching (Jia et al., 2016; Barbosa et al., 2018). This phosphosite is upregulated by TCSA, potentially impeding *de novo* SAM formation by diminishing auxin maxima. *MPK3/6* are also downstream of *YDA*, which is inhibited by *BIN2*-mediated phosphorylation (Kim et al., 2012). As *BIN2* harbors a downregulated tyrosine (Y200) and autophosphorylation of this site is positively correlated with kinase activity (Li et al., 2020), *BIN2* could act upstream of differential *PIN* phosphorylation in TCSA responses. Moreover, *BIN2* is involved in auxin signaling and enhances induction of *LBD16* and *LBD29* by *ARF7* and *ARF19* during lateral rooting, which is also required for callus formation (Vert et al., 2008; Cho et al., 2013; Lee and Seo, 2017; Lardon and Geelen, 2020). On the other hand, the *MPK3/6* module normally promotes embryonic patterning (Neu et al., 2019), and *BIN2* suppresses *BR* signaling by phosphorylation-dependent degradation of *BZR1*, which is linked to reduced proliferation and regeneration (He et al., 2002; Cheon et al., 2010). Hence, the contribution of *BIN2* to impaired shoot formation by TCSA is ambiguous.

*BR*s also control the formation of organ boundaries *via* *CUC*s (Gendron et al., 2012), and additional *BR* signaling factors containing TCSA-responsive DRPs are *BSL1* and *BSL3* (Kim et al., 2016), *BSK5* (Li et al., 2012), *GF14 PHI* (interacting with *BZR1* [Ryu

et al., 2007)], and TPR2 [a homolog of the TOPLESS corepressor involved in auxin and BR responses, as well as SAM specification (Long et al., 2006; Espinosa-Ruiz et al., 2017; Martín-Arevalillo et al., 2017)]. Interestingly, BR-induced gene expression is modulated *via* selective autophagy of BES1 (requiring phosphorylation of DSK2 by BIN2; Nolan et al., 2017) and TCSA affects phosphosites in autophagy-related proteins (e.g., ATG1B, ATG1C, ATG3, ATG13A, and ATG18F). Moreover, ATEH1 and ATG13A phosphopeptides are not detected after TCSA treatment (Supplementary Table 1) and ATEH1 interacts with PVA11/VAP27-1 (containing two DRPs) at ER-PM contact sites to mediate endocytosis and autophagosome biogenesis (Wang et al., 2019a). Intriguingly, autophagy is required for proteome adjustments during hormone-induced reprogramming of somatic cells to pluripotent stem cells and subsequent redifferentiation (Rodríguez et al., 2020), providing an additional mechanism for TCSA-impaired shoot organogenesis. Besides, ATG8 proteins show interplay with cytokinin-regulated root architecture (Slavikova et al., 2008) and numerous genes are transcriptionally coregulated in *atg*, *ahk2 ahk3 ahk4*, and *arr1 arr10 arr12* mutants (Masclaux-Daubresse et al., 2014). The GSEA network also contains several exocyst subunits (e.g., EXO70D2, EXO70H7, SEC1B, and SEC5A), which promote autophagic degradation of A-type ARRs upon phosphorylation of a conserved D residue in the receiver domain to tweak CK sensitivity in response to carbon starvation (Acheampong et al., 2020). Whether this could also regulate B-type ARRs, such as ARR1, remains to be investigated.

In summary, the salicylanilide TCSA impairs shoot regeneration from roots when applied during the first 4 days of SIM incubation. Genetic analyses suggest that this is at least partially caused by interference with histidine kinases and phosphotransfer proteins involved in cytokinin signal transduction, such as AHK3, AHK4, AHP3, and AHP5. Phosphoproteomics further reveals profound deregulation of Ser/Thr/Tyr phosphorylation, which affects factors linked to protein modification, transcriptional regulation, vesicle trafficking, organ morphogenesis, and cation transport. Further research on TCSA-responsive phosphoproteins such as AGO1, BAM1, PLL5, PIN1, and BIN2, will determine whether these are direct targets or act downstream of the CK shoot induction pathway.

## Data availability statement

The raw data generated in this study can be found in the PRIDE repository with identifier PXD030754. Processed results of the phosphoproteome analysis are available in Supplementary Data 1.

## References

- Acheampong, A. K., Shanks, C., Cheng, C. Y., Eric Schaller, G., Dagdas, Y., and Kieber, J. J. (2020). EXO70D isoforms mediate selective autophagic degradation of type-A ARR proteins to regulate cytokinin sensitivity. *Proc. Natl. Acad. Sci. U. S. A.* 117, 27034–27043. doi: 10.1073/PNAS.2013161117
- Albert, E. V., Kawai-ool, U. N., and Ezhova, T. A. (2015). Pleiotropic effect of the *fas5* mutation on the shoot development of *Arabidopsis thaliana*. *Russ. J. Dev. Biol.* 461, 10–18. doi: 10.1134/S1062360415010038

## Author contributions

RL designed and performed experiments, analyzed and visualized data, and wrote the manuscript. HT and BC helped with experiments. XX and LV assisted in data analysis. MP provided resources. SV edited the manuscript. DG and IDS conceptualized research, supervised the project, and edited the manuscript. All authors contributed to the article and approved the submitted version.

## Funding

This work was supported by the Research Foundation Flanders (FWO; application numbers 1S48517N and G094619N).

## Acknowledgments

We thank Biobix members Steven Verbruggen, Marlies Peeters, Jeroen Galle, and Wim Van Crieking for the use of their server and advice on computational phosphoproteomics. Plant Sciences Core Facility of CEITEC Masaryk University is acknowledged for the technical support.

## Conflict of interest

The authors declare that the research was conducted in the absence of any commercial or financial relationships that could be construed as a potential conflict of interest.

## Publisher's note

All claims expressed in this article are solely those of the authors and do not necessarily represent those of their affiliated organizations, or those of the publisher, the editors and the reviewers. Any product that may be evaluated in this article, or claim that may be made by its manufacturer, is not guaranteed or endorsed by the publisher.

## Supplementary material

The Supplementary material for this article can be found online at: <https://www.frontiersin.org/articles/10.3389/fpls.2022.894208/full#supplementary-material>

- Ashburner, M., Ball, C. A., Blake, J. A., Botstein, D., Butler, H., Cherry, J. M., et al. (2000). Gene ontology: tool for the unification of biology. The gene ontology consortium. *Nat. Genet.* 25, 25–29. doi: 10.1038/75556

- Avraham, S., Tung, C.-W., Ilic, K., Jaiswal, P., Kellogg, E. A., McCouch, S., et al. (2008). The plant ontology database: a community resource for plant structure and developmental stages controlled vocabulary and annotations. *Nucleic Acids Res.* 36, D449–D454. doi: 10.1093/nar/gkm908

- Barbez, E., Kubeš, M., Rolčík, J., Béziat, C., Pěnčík, A., Wang, B., et al. (2012). A novel putative auxin carrier family regulates intracellular auxin homeostasis in plants. *Nature* 485, 119–122. doi: 10.1038/nature11001
- Barbosa, I. C. R., Hammes, U. Z., and Schwechheimer, C. (2018). Activation and polarity control of PIN-FORMED Auxin transporters by phosphorylation. *Trends Plant Sci.* 23, 523–538. doi: 10.1016/j.TPLANTS.2018.03.009
- Bell, E. M., Lin, W. C., Husbands, A. Y., Yu, L., Jaganatha, V., Jablonska, B., et al. (2012). Arabidopsis lateral organ boundaries negatively regulates brassinosteroid accumulation to limit growth in organ boundaries. *Proc. Natl. Acad. Sci. U. S. A.* 109, 21146–21151. doi: 10.1073/pnas.1210789109
- Bentem, S., Anrather, D., Dohnal, I., Roitingner, E., Csaszar, E., Joore, J., et al. (2008). Site-specific phosphorylation profiling of Arabidopsis proteins by mass spectrometry and peptide Chip analysis. *J. Proteome Res.* 7, 2458–2470. doi: 10.1021/PR8000173
- Bindea, G., Galon, J., and Mlecnik, B. (2013). CluePedia Cytoscape plugin: pathway insights using integrated experimental and *in silico* data. *Bioinformatics* 29, 661–663. doi: 10.1093/bioinformatics/btt019
- Bindea, G., Mlecnik, B., Hackl, H., Charoentong, P., Tosolini, M., Kirilovsky, A., et al. (2009). Clue GO: a Cytoscape plug-in to decipher functionally grouped gene ontology and pathway annotation networks. *Bioinformatics* 25, 1091–1093. doi: 10.1093/bioinformatics/btp101
- Blackwell, H. E., and Zhao, Y. (2003). Chemical genetic approaches to plant biology. *Plant Physiol.* 133, 448–455. doi: 10.1104/pp.103.031138
- Bustillo-Avendaño, E., Ibáñez, S., Sanz, O., Barros, J. A. S., Gude, I., Perianez-Rodríguez, J., et al. (2018). Regulation of hormonal control, cell reprogramming, and patterning during *de novo* root organogenesis. *Plant Physiol.* 176, 1709–1727. doi: 10.1104/pp.17.00980
- Cerny, M., Dycka, F., Bobál'ová, J., and Brzobohaty, B. (2011). Early cytokinin response proteins and phosphoproteins of *Arabidopsis thaliana* identified by proteome and phosphoproteome profiling. *J. Exp. Bot.* 62, 921–937. doi: 10.1093/jxb/erq322
- Chang, W., Guo, Y., Zhang, H., Liu, X., and Guo, L. (2020). Same actor in different stages: genes in shoot apical meristem maintenance and floral meristem determinacy in Arabidopsis. *Front. Ecol. Evol.* 8:89. doi: 10.3389/FEVO.2020.00089
- Chatfield, S. P., and Raizada, M. N. (2008). Ethylene and shoot regeneration: hookless1 modulates *de novo* shoot organogenesis in *Arabidopsis thaliana*. *Plant Cell Rep.* 27, 655–666. doi: 10.1007/s00299-007-0496-3
- Chen, Y. M., Ferrar, T. S., Lohmeir-Vogel, E., Morrice, N., Mizuno, Y., Berenger, B., et al. (2006). The PII signal transduction protein of *Arabidopsis thaliana* forms an arginine-regulated complex with plastid N-acetyl glutamate kinase. *J. Biol. Chem.* 281, 5726–5733. doi: 10.1074/JBC.M510945200
- Cheon, J., Park, S. Y., Schulz, B., and Choe, S. (2010). Arabidopsis brassinosteroid biosynthetic mutant dwarf7–1 exhibits slower rates of cell division and shoot induction. *BMC Plant Biol.* 10:270. doi: 10.1186/1471-2229-10-270
- Chevalier, D., Batoux, M., Fulton, L., Pfister, K., Yadav, R. K., Schellenberg, M., et al. (2005). STRUBBELIG defines a receptor kinase-mediated signaling pathway regulating organ development in Arabidopsis. *Proc. Natl. Acad. Sci. U. S. A.* 102, 9074–9079. doi: 10.1073/pnas.0503526102
- Chitteti, B. R., and Peng, Z. (2007). Proteome and phosphoproteome dynamic change during cell dedifferentiation in Arabidopsis. *Proteomics* 7, 1473–1500. doi: 10.1002/pmic.200600871
- Cho, M., Lee, Z.-W., and Cho, H.-T. (2012). ATP-binding cassette B4, an Auxin-efflux transporter, stably associates with the plasma membrane and shows distinctive intracellular trafficking from That of PIN-FORMED proteins. *Plant Physiol.* 159, 642–654. doi: 10.1104/PP.112.196139
- Cho, H., Ryu, H., Rho, S., Hill, K., Smith, S., Audenaert, D., et al. (2013, 2013). A secreted peptide acts on BIN2-mediated phosphorylation of ARFs to potentiate auxin response during lateral root development. *Nat. Cell Biol.* 16, 66–76. doi: 10.1038/ncb2893
- Cox, J., and Mann, M. (2008). MaxQuant enables high peptide identification rates, individualized p.p.b.-range mass accuracies and proteome-wide protein quantification. *Nat. Biotechnol.* 26, 1367–1372. doi: 10.1038/nbt.1511
- Dautel, R., Wu, X. N., Heunemann, M., Schulze, W. X., and Harter, K. (2016). The Sensor Histidine kinases AHK2 and AHK3 proceed into multiple serine/threonine/tyrosine phosphorylation pathways in *Arabidopsis thaliana*. *Mol. Plant* 9, 182–186. doi: 10.1016/j.molp.2015.10.002
- De Rybel, B., Audenaert, D., Vert, G., Rozhon, W., Mayerhofer, J., Peelman, F., et al. (2009). Chemical inhibition of a subset of *Arabidopsis thaliana* GSK3-like kinases activates Brassinosteroid signaling. *Chem. Biol.* 16, 594–604. doi: 10.1016/j.chembiol.2009.04.008
- De Smet, I., Vassileva, V., De Rybel, B., Levesque, M. P., Grunewald, W., Van Damme, D., et al. (2008). Receptor-like kinase ACR4 restricts formative cell divisions in the Arabidopsis root. *Science* 322, 594–597. doi: 10.1126/science.1160158
- Deng, K., Dong, P., Wang, W., Feng, L., Xiong, F., Wang, K., et al. (2017). The TOR pathway is involved in adventitious root formation in Arabidopsis and potato. *Front. Plant Sci.* 8:784. doi: 10.3389/fpls.2017.00784
- Deng, K., Yu, L., Zheng, X., Zhang, K., Wang, W., Dong, P., et al. (2016). Target of rapamycin is a key player for auxin signaling transduction in Arabidopsis. *Front. Plant Sci.* 7:291. doi: 10.3389/fpls.2016.00291
- Desikan, R., Horák, J., Chaban, C., Mira-Rodado, V., Witthöft, J., Elgass, K., et al. (2008). The histidine kinase AHK5 integrates endogenous and environmental signals in Arabidopsis guard cells. *PLoS One* 3:e2491. doi: 10.1371/journal.pone.0002491
- DeYoung, B. J., Bickle, K. L., Schrage, K. J., Muskett, P., Patel, K., and Clark, S. E. (2006). The CLAVATA1-related BAM1, BAM2 and BAM3 receptor kinase-like proteins are required for meristem function in Arabidopsis. *Plant J.* 45, 1–16. doi: 10.1111/j.1365-313X.2005.02592.x
- DeYoung, B. J., and Clark, S. E. (2008). BAM receptors regulate stem cell specification and organ development Through complex interactions With CLAVATA signaling. *Genetics* 180, 895–904. doi: 10.1534/GENETICS.108.091108
- Dhonukshe, P., Aniento, F., Hwang, I., Robinson, D. G., Mravec, J., Stierhof, Y. D., et al. (2007). Clathrin-mediated constitutive endocytosis of PIN Auxin efflux carriers in Arabidopsis. *Curr. Biol.* 17, 520–527. doi: 10.1016/j.cub.2007.01.052
- Du, F., Gong, W., Boscá, S., Tucker, M., Vaucheret, H., and Laux, T. (2020). Dose-dependent AGO1-mediated inhibition of the miRNA165/166 pathway modulates stem cell maintenance in Arabidopsis shoot apical meristem. *Plant Commun.* 1:100002. doi: 10.1016/j.XPLC.2019.100002
- Espinosa-Ruiz, A., Martínez, C., De Lucas, M., Fabregas, N., Bosch, N., Cano-Delgado, A. I., et al. (2017). TOPLESS mediates brassinosteroid control of shoot boundaries and root meristem development in *Arabidopsis thaliana*. *Development* 144, 1619–1628. doi: 10.1242/dev.143214
- Fendrych, M., Leung, J., and Friml, J. (2016). Tir1/AFB-aux/IAA auxin perception mediates rapid cell wall acidification and growth of Arabidopsis hypocotyls. *Elife* 5:e19048. doi: 10.7554/ELIFE.19048
- Fuglsang, A. T., Guo, Y., Cui, T. A., Qiu, Q., Song, C., Kristiansen, K. A., et al. (2007). Arabidopsis protein kinase PKS5 inhibits the plasma membrane H<sup>+</sup>-ATPase by preventing interaction with 14-3-3 protein. *Plant Cell* 19, 1617–1634. doi: 10.1105/TPC.105.035626
- Fuglsang, A. T., Visconti, S., Drumm, K., Jahn, T., Stensballe, A., Mattei, B., et al. (1999). Binding of 14-3-3 protein to the plasma membrane H<sup>+</sup>-ATPase AH2 involves the three C-terminal residues Tyr946-Thr-Val and requires phosphorylation of Thr947. *J. Biol. Chem.* 274, 36774–36780. doi: 10.1074/JBC.274.51.36774
- Fulton, L., Batoux, M., Vaddepalli, P., Yadav, R. K., Busch, W., Andersen, S. U., et al. (2009). DETORQUEO, QUIRKY, and ZERZAUST represent novel components involved in organ development mediated by the receptor-like kinase STRUBBELIG in *Arabidopsis thaliana*. *PLoS Genet.* 5:e1000355. doi: 10.1371/journal.pgen.1000355
- Gan, X., Stegle, O., Behr, J., Steffen, J. G., Drewe, P., Hildebrand, K. L., et al. (2011). Multiple reference genomes and transcriptomes for *Arabidopsis thaliana*. *Nature*, 419–423. doi: 10.1038/nature10414
- Gendron, J. M., Liu, J. S., Fan, M., Bai, M. Y., Wenkel, S., Springer, P. S., et al. (2012). Brassinosteroids regulate organ boundary formation in the shoot apical meristem of Arabidopsis. *Proc. Natl. Acad. Sci. U. S. A.* 109, 21152–21157. doi: 10.1073/pnas.1210799110
- González-García, M. P., Vilarrasa-Blasi, J., Zhiponova, M., Divol, F., Mora-García, S., Russinova, E., et al. (2011). Brassinosteroids control meristem size by promoting cell cycle progression in Arabidopsis roots. *Development* 138, 849–859. doi: 10.1242/dev.057331
- Graf, P., Dolzblas, A., Würschum, T., Lenhard, M., Pfreundt, U., and Laux, T. (2010). MGOON1 encodes an Arabidopsis type IB DNA topoisomerase required in stem cell regulation and to maintain developmentally regulated gene silencing. *Plant Cell* 22, 716–728. doi: 10.1105/TPC.109.068296
- Groen, A. J., Sancho-Andrés, G., Breckels, L. M., Gatto, L., Aniento, F., and Lilley, K. S. (2014). Identification of trans-Golgi network proteins in *Arabidopsis thaliana* root tissue. *J. Proteome Res.* 13, 763–776. doi: 10.1021/PR4008464
- Gu, Z., Eils, R., and Schlesner, M. (2016). Complex heatmaps reveal patterns and correlations in multidimensional genomic data. *Bioinformatics* 32, 2847–2849. doi: 10.1093/BIOINFORMATICS/BTW313
- Hager, A., Debus, G., Edel, H. G., Stransky, H., and Serrano, R. (1991). Auxin induces exocytosis and the rapid synthesis of a high-turnover pool of plasma-membrane H<sup>+</sup>-ATPase. *Planta* 185, 527–537. doi: 10.1007/BF00202963
- Haruta, M., Burch, H. L., Nelson, R. B., Barrett-Wilt, G., Kline, K. G., Mohsin, S. B., et al. (2010). Molecular characterization of mutant Arabidopsis plants with reduced plasma membrane proton pump activity. *J. Biol. Chem.* 285, 17918–17929. doi: 10.1074/JBC.M110.101733
- Haruta, M., and Sussman, M. R. (2012). The effect of a genetically reduced plasma membrane Protonmotive force on vegetative growth of Arabidopsis. *Plant Physiol.* 158, 1158–1171. doi: 10.1104/PP.111.189167

- He, J.-X., Gendron, J. M., Yang, Y., Li, J., and Wang, Z.-Y. (2002). The GSK3-like kinase BIN2 phosphorylates and destabilizes BZR1, a positive regulator of the brassinosteroid signaling pathway in Arabidopsis. *Proc. Natl. Acad. Sci.* 99, 10185–10190. doi: 10.1073/PNAS.152342599
- Heerah, S., Molinari, R., Guerrier, S., and Marshall-Colon, A. (2021). Granger-causal testing for irregularly sampled time series with application to nitrogen signalling in Arabidopsis. *Bioinformatics* 37, 2450–2460. doi: 10.1093/BIOINFORM/BTAB126
- Heyl, A., Ramireddy, E., Brenner, W. G., Riefler, M., Allemeersch, J., and Schmülling, T. (2008). The transcriptional repressor ARR1-SRDX suppresses pleiotropic cytokinin activities in Arabidopsis. *Plant Physiol.* 147, 1380–1395. doi: 10.1104/pp.107.115436
- Hicks, G. R., and Raikhel, N. V. (2012). Small molecules present large opportunities in plant biology. *Annu. Rev. Plant Biol.* 63, 261–282. doi: 10.1146/annurev-arplant-042811-105456
- Hicks, G. R., and Raikhel, N. V. (2014). Plant chemical biology: are we meeting the promise? *Front. Plant Sci.* 5:455. doi: 10.3389/fpls.2014.00455
- Higuchi, M., Pischke, M. S., Mähönen, A. P., Miyawaki, K., Hashimoto, Y., Seki, M., et al. (2004). In planta functions of the Arabidopsis cytokinin receptor family. *Proc. Natl. Acad. Sci. U. S. A.* 101, 8821–8826. doi: 10.1073/pnas.0402887101
- Hsieh, M.-H., Lam, H.-M., Loo, F. J., and Coruzzi, G. (1998). A PII-like protein in Arabidopsis: putative role in nitrogen sensing. *Proc. Natl. Acad. Sci.* 95, 13965–13970. doi: 10.1073/PNAS.95.23.13965
- Hsu, J.-L., Wang, L.-Y., Wang, S.-Y., Lin, C.-H., Ho, K.-C., Shi, F.-K., et al. (2009). Functional phosphoproteomic profiling of phosphorylation sites in membrane fractions of salt-stressed *Arabidopsis thaliana*. *Proteome Sci.* 7, 1–16. doi: 10.1186/1477-5956-7-42
- Huang, X., Hou, L., Meng, J., You, H., Li, Z., Gong, Z., et al. (2018). The antagonistic action of Abscisic acid and Cytokinin signaling mediates drought stress response in Arabidopsis. *Mol. Plant* 11, 970–982. doi: 10.1016/J.MOLP.2018.05.001
- Huang, R., Shu, S., Liu, M., Wang, C., Jiang, B., Jiang, J., et al. (2019a). Nuclear Prohibitin3 maintains genome integrity and cell proliferation in the root meristem through Minichromosome maintenance 2. *Plant Physiol.* 179, 1669–1691. doi: 10.1104/PP.18.01463
- Huang, R., Zheng, R., He, J., Zhou, Z., Wang, J., Xiong, Y., et al. (2019b). Noncanonical auxin signaling regulates cell division pattern during lateral root development. *Proc. Natl. Acad. Sci. U. S. A.* 116, 21285–21290. doi: 10.1073/pnas.1910916116
- Hwang, I., Chen, H. C., and Sheen, J. (2002). Two-component signal transduction pathways in Arabidopsis. *Plant Physiol.* 129, 500–515. doi: 10.1104/pp.005504
- Ikeuchi, M., Favero, D. S., Sakamoto, Y., Iwase, A., Coleman, D., Rymen, B., et al. (2019). Molecular mechanisms of plant regeneration. *Annu. Rev. Plant Biol.* 70, 377–406. doi: 10.1146/annurev-arplant-050718-100434
- Ikeuchi, M., Ogawa, Y., Iwase, A., and Sugimoto, K. (2016). Plant regeneration: cellular origins and molecular mechanisms. *Development* 143, 1442–1451. doi: 10.1242/dev.134668
- Jeon, J., and Kim, J. (2013). Arabidopsis response regulator1 and Arabidopsis histidine phosphotransfer protein2 (AHP2), AHP3, and AHP5 function in cold signaling. *Plant Physiol.* 161, 408–424. doi: 10.1104/pp.112.207621
- Jeon, J., Kim, N. Y., Kim, S., Kang, N. Y., Novák, O., Ku, S. J., et al. (2010). A subset of cytokinin two-component signaling system plays a role in cold temperature stress response in Arabidopsis. *J. Biol. Chem.* 285, 23371–23386. doi: 10.1074/jbc.M109.096644
- Jia, W., Li, B., Li, S., Liang, Y., Wu, X., Ma, M., et al. (2016). Mitogen-activated protein kinase Cascade MKK7-MPK6 plays important roles in plant development and regulates shoot branching by phosphorylating PIN1 in Arabidopsis. *PLoS Biol.* 14:e1002550. doi: 10.1371/JOURNAL.PBIO.1002550
- Kakimoto, T. (1996). CKII, a Histidine kinase homolog implicated in Cytokinin signal transduction. *Science* 274, 982–985. doi: 10.1126/SCIENCE.274.5289.982
- Kanehisa, M., and Goto, S. (2000). KEGG: Kyoto encyclopedia of genes and genomes. *Nucleic Acids Res.* 28, 27–30. doi: 10.1093/nar/28.1.27
- Kidner, C. A., and Martienssen, R. A. (2005). The role of ARGONAUTE1 (AGO1) in meristem formation and identity. *Dev. Biol.* 280, 504–517. doi: 10.1016/J.YDBIO.2005.01.031
- Kieber, J. J., and Schaller, G. E. (2018). Cytokinin signaling in plant development. *Development* 145:dev149344. doi: 10.1242/dev.149344
- Kim, T. W., Michniewicz, M., Bergmann, D. C., and Wang, Z. Y. (2012). Brassinosteroid regulates stomatal development by GSK3-mediated inhibition of a MAPK pathway. *Nature* 482, 419–422. doi: 10.1038/nature10794
- Kim, E.-J., Youn, J.-H., Park, C.-H., Kim, T.-W., Guan, S., Xu, S., et al. (2016). Oligomerization between BSU1 Family Members Potentiates Brassinosteroid Signaling in Arabidopsis. *Mol. Plant* 9, 178–181. doi: 10.1016/j.molp.2015.09.012
- Kinoshita, T., and Shimazaki, K. (1999). Blue light activates the plasma membrane H(+)-ATPase by phosphorylation of the C-terminus in stomatal guard cells. *EMBO J.* 18, 5548–5558. doi: 10.1093/EMBOJ/18.20.5548
- Kitakura, S., Vanneste, S., Robert, S., Löffke, C., Teichmann, T., Tanaka, H., et al. (2011). Clathrin mediates endocytosis and polar distribution of PIN auxin transporters in Arabidopsis. *Plant Cell* 23, 1920–1931. doi: 10.1105/tpc.111.083030
- Kurepa, J., Li, Y., Perry, S. E., and Smalle, J. A. (2014a). Ectopic expression of the phosphomimic mutant version of Arabidopsis response regulator 1 promotes a constitutive cytokinin response phenotype. *BMC Plant Biol.* 14:28. doi: 10.1186/1471-2229-14-28
- Kurepa, J., Li, Y., and Smalle, J. A. (2014b). Cytokinin signaling stabilizes the response activator ARR1. *Plant J.* 78, 157–168. doi: 10.1111/TPJ.12458
- Lardon, R., and Geelen, D. (2020). Natural variation in plant Pluripotency and regeneration. *Plan. Theory* 9:1261. doi: 10.3390/plants9101261
- Lardon, R., Wijnker, E., Keurentjes, J., and Geelen, D. (2020). The genetic framework of shoot regeneration in Arabidopsis comprises master regulators and conditional fine-tuning factors. *Commun. Biol.* 3:549. doi: 10.1038/s42003-020-01274-9
- Laufs, P., Peaucelle, A., Morin, H., and Traas, J. (2004). MicroRNA regulation of the CUC genes is required for boundary size control in Arabidopsis meristems. *Development* 131, 4311–4322. doi: 10.1242/DEV.01320
- Lee, K., and Seo, P. J. (2017). High-temperature promotion of callus formation requires the BIN2-ARF-LBD axis in Arabidopsis. *Planta* 246, 797–802. doi: 10.1007/s00425-017-2747-z
- Li, H., Cai, Z., Wang, X., Li, M., Cui, Y., Cui, N., et al. (2019). SERK receptor-like kinases control division patterns of vascular precursors and ground tissue stem cells during embryo development in Arabidopsis. *Mol. Plant* 12, 984–1002. doi: 10.1016/j.molp.2019.04.011
- Li, J., Terzaghi, W., Gong, Y., Li, C., Ling, J.-J., Fan, Y., et al. (2020). Modulation of BIN2 kinase activity by HY5 controls hypocotyl elongation in the light. *Nat. Commun.* 11, 1592–1511. doi: 10.1038/s41467-020-15394-7
- Liu, Z., Dai, X., Li, J., Liu, N., Liu, X., Li, S., et al. (2020). The type-B cytokinin response regulator ARR1 inhibits shoot regeneration in an ARR12-dependent manner in Arabidopsis. *Plant Cell* 32, 2271–2291. doi: 10.1105/tpc.19.00022
- Liu, X., Gao, L., Dinh, T. T., Shi, T., Li, D., Wang, R., et al. (2014). DNA topoisomerase I affects Polycomb group protein-mediated epigenetic regulation and plant development by altering nucleosome distribution in Arabidopsis. *Plant Cell* 26, 2803–2817. doi: 10.1105/TPC.114.124941
- Liu, L., Li, C., Song, S., Teo, Z. W. N., Shen, L., Wang, Y., et al. (2018). FTIP-dependent STM trafficking regulates shoot meristem development in Arabidopsis. *Cell Rep.* 23, 1879–1890. doi: 10.1016/j.celrep.2018.04.033
- Liu, Q., Yao, X., Pi, L., Wang, H., Cui, X., and Huang, H. (2009). The ARGONAUTE10 gene modulates shoot apical meristem maintenance and establishment of leaf polarity by repressing miR165/166 in Arabidopsis. *Plant J.* 58, 27–40. doi: 10.1111/J.1365-313X.2008.03757.X
- Long, J. A., Ohno, C., Smith, Z. R., and Meyerowitz, E. M. (2006). TOPLESS regulates apical embryonic fate in Arabidopsis. *Science* 312, 1520–1523. doi: 10.1126/SCIENCE.1123841
- Lozano-Elena, F., Planas-Riverola, A., Vilarrasa-Blasi, J., Schwab, R., and Caño-Delgado, A. I. (2018). Paracrine brassinosteroid signaling at the stem cell niche controls cellular regeneration. *J. Cell Sci.* 131:jcs204065. doi: 10.1242/jcs.204065
- Marhavý, P., Bielach, A., Abas, L., Abuzeineh, A., Duclercq, J., Tanaka, H., et al. (2011). Cytokinin modulates Endocytic trafficking of PIN1 Auxin efflux carrier to control plant organogenesis. *Dev. Cell* 21, 796–804. doi: 10.1016/j.devcel.2011.08.014
- Martin-Arevalillo, R., Nanao, M. H., Larriue, A., Vinos-Poyo, T., Mast, D., Galvan-Ampudia, C., et al. (2017). Structure of the Arabidopsis TOPLESS corepressor provides insight into the evolution of transcriptional repression. *Proc. Natl. Acad. Sci. U. S. A.* 114, 8107–8112. doi: 10.1073/PNAS.1703054114
- Masclaux-Daubresse, C., Clément, G., Anne, P., Routaboul, J. M., Guiboileau, A., Soulay, F., et al. (2014). Stitching together the multiple dimensions of autophagy using metabolomics and Transcriptomics reveals impacts on metabolism, development, and plant responses to the environment in Arabidopsis. *Plant Cell* 26, 1857–1877. doi: 10.1105/TPC.114.124677
- Mccourt, P., and Desveaux, D. (2010). Plant chemical genetics. *New Phytol.* 185, 15–26. doi: 10.1111/j.1469-8137.2009.03045.x
- McCready, K., Spencer, V., and Kim, M. (2020). The importance of TOR kinase in plant development. *Front. Plant Sci.* 11:16. doi: 10.3389/fpls.2020.00016
- Menand, B., Desnos, T., Nussaume, L., Bergert, F., Bouchez, D., Meyer, C., et al. (2002). Expression and disruption of the Arabidopsis TOR (target of rapamycin) gene. *Proc. Natl. Acad. Sci. U. S. A.* 99, 6422–6427. doi: 10.1073/pnas.092141899
- Méndez-Hernández, H. A., Ledezma-Rodríguez, M., Avilez-Montalvo, R. N., Juárez-Gómez, Y. L., Skeete, A., Avilez-Montalvo, J., et al. (2019). Signaling

- overview of plant somatic embryogenesis. *Front. Plant Sci.* 10:7. doi: 10.3389/fpls.2019.00077
- Meng, W. J., Cheng, Z. J., Sang, Y. L., Zhang, M. M., Rong, X. F., Wang, Z. W., et al. (2017). Type-B ARABIDOPSIS RESPONSE REGULATORS specify the shoot stem cell niche by dual regulation of WUSCHEL. *Plant Cell* 29, 1357–1372. doi: 10.1105/tpc.16.00640
- Meng, X., Wang, H., He, Y., Liu, Y., Walker, J. C., Torii, K. U., et al. (2013). A MAPK cascade downstream of ERECTA receptor-like protein kinase regulates Arabidopsis inflorescence architecture by promoting localized cell proliferation. *Plant Cell* 24, 4948–4960. doi: 10.1105/tpc.112.104695
- Motte, H., Vercauteren, A., Depuydt, S., Landschoot, S., Geelen, D., Werbrouck, S., et al. (2014a). Combining linkage and association mapping identifies RECEPTOR-LIKE PROTEIN KINASE1 as an essential Arabidopsis shoot regeneration gene. *Proc. Natl. Acad. Sci. U. S. A.* 111, 8305–8310. doi: 10.1073/pnas.1404978111
- Motte, H., Vereecke, D., Geelen, D., and Werbrouck, S. (2014b). The molecular path to in vitro shoot regeneration. *Biotechnol. Adv.* 32, 107–121. doi: 10.1016/j.biotechadv.2013.12.002
- Neu, A., Eilbert, E., Asseck, L. Y., Slane, D., Henschen, A., Wang, K., et al. (2019). Constitutive signaling activity of a receptor-associated protein links fertilization with embryonic patterning in *Arabidopsis thaliana*. *Proc. Natl. Acad. Sci. U. S. A.* 116, 5795–5804. doi: 10.1073/pnas.1815866116
- Ni, D. A., Sozzani, R., Blanchet, S., Domenichini, S., Reuzeau, C., Cella, R., et al. (2009). The Arabidopsis MCM2 gene is essential to embryo development and its over-expression alters root meristem function. *New Phytol.* 184, 311–322. doi: 10.1111/j.1469-8137.2009.02961.x
- Nishimura, C., Ohashi, Y., Sato, S., Kato, T., Tabata, S., and Ueguchi, C. (2004). Histidine kinase homologs that act as cytokinin receptors possess overlapping functions in the regulation of shoot and root growth in arabidopsis. *Plant Cell* 16, 1365–1377. doi: 10.1105/tpc.021477
- Nolan, T. M., Brennan, B., Yang, M., Chen, J., Zhang, M., Li, Z., et al. (2017). Selective autophagy of BES1 mediated by DSK2 balances plant growth and survival. *Dev. Cell* 41, 33.e7–46.e7. doi: 10.1016/j.devcel.2017.03.013
- Nongpiur, R., Soni, P., Karan, R., Singla-Pareek, S. L., and Pareek, A. (2012). Histidine kinases in plants: cross talk between hormone and stress responses. *Plant Signal. Behav.* 7, 1230–1237. doi: 10.4161/psb.21516
- Noutoshi, Y., Kuromori, T., Wada, T., Hirayama, T., Kamiya, A., Imura, Y., et al. (2006). Loss of NECROTIC SPOTTED LESIONS 1 associates with cell death and defense responses in *Arabidopsis thaliana*. *Plant Mol. Biol.* 62, 29–42. doi: 10.1007/S11103-006-9001-6
- Ötvös, K., Miskolczi, P., Marhavý, P., Cruz-Ramírez, A., Benková, E., Robert, S., et al. (2021). Pickle recruits Retinoblastoma related 1 to control lateral root formation in Arabidopsis. *Int. J. Mol. Sci.* 22:3862. doi: 10.3390/IJMS22083862
- Pacifici, E., Mambro, R., Ioio, R., Costantino, P., and Sabatini, S. (2018). Acidic cell elongation drives cell differentiation in the Arabidopsis root. *EMBO J.* 37:e99134. doi: 10.15252/EMBJ.201899134
- Papon, N., Clastre, M., Gantet, P., Rideau, M., Chénieux, J.-C., and Crèche, J. (2003). Inhibition of the plant cytokinin transduction pathway by bacterial histidine kinase inhibitors in *Catharanthus roseus* cell cultures. *FEBS Lett.* 537, 5–101. doi: 10.1016/S0014-5793(03)00102-9
- Papon, N., Senoussi, M. M., Andreu, F., Rideau, M., Chenieux, J. C., and Creche, J. (2004). Cloning of a gene encoding a putative ethylene receptor in *Catharanthus roseus* and its expression in plant and cell cultures. *Biol. Plant.* 48, 345–350. doi: 10.1023/B:BIOP.0000041085.82296.9c
- Park, C. J., Caddell, D. F., and Ronald, P. C. (2012). Protein phosphorylation in plant immunity: insights into the regulation of pattern recognition receptor-mediated signaling. *Front. Plant Sci.* 3:177. doi: 10.3389/fpls.2012.00177
- Perez-Riverol, Y., Csordas, A., Bai, J., Bernal-Llinares, M., Hewapathirana, S., Kundu, D. J., et al. (2019). The PRIDE database and related tools and resources in 2019: improving support for quantification data. *Nucleic Acids Res.* 47, D442–D450. doi: 10.1093/NAR/GKY1106
- Perilli, S., Perez-Perez, J. M., Mambro, R., Peris, C. L., Díaz-Triviño, S., Bianco, M., et al. (2013). RETINOBLASTOMA-RELATED protein stimulates cell differentiation in the Arabidopsis root meristem by interacting with Cytokinin signaling. *Plant Cell* 25, 4469–4478. doi: 10.1105/TPC.113.116632
- Pernisova, M., Grochova, M., Konecny, T., Plackova, L., Harustiaková, D., Kakimoto, T., et al. (2018). Cytokinin signalling regulates organ identity via the AHK4 receptor in arabidopsis. *Development* 145:dev163907. doi: 10.1242/dev.163907
- Ren, M., Venglat, P., Qiu, S., Feng, L., Cao, Y., Wang, E., et al. (2012). Target of rapamycin signaling regulates metabolism, growth, and life span in Arabidopsis. *Plant Cell* 24, 4850–4874. doi: 10.1105/tpc.112.107144
- Riefler, M., Novak, O., Strnad, M., and Schmülling, T. (2006). Arabidopsis Cytokinin receptor mutants reveal functions in shoot growth, leaf senescence, seed size, germination, root development, and Cytokinin metabolism. *Plant Cell* 18, 40–54. doi: 10.1105/TPC.105.037796
- Ritchie, M. E., Phipson, B., Wu, D., Hu, Y., Law, C. W., Shi, W., et al. (2015). Limma powers differential expression analyses for RNA-seq and microarray studies. *Nucleic Acids Res.* 43:e47. doi: 10.1093/nar/gkv007
- Rodriguez, E., Chevalier, J., Olsen, J., Ansøl, J., Kapousidou, V., Zuo, Z., et al. (2020). Autophagy mediates temporary reprogramming and dedifferentiation in plant somatic cells. *EMBO J.* 39:e103315. doi: 10.15252/EMBJ.2019103315
- Ross, A. R. S. (2007). “Identification of Histidine Phosphorylations in proteins using mass spectrometry and affinity-based techniques,” in *Methods in Enzymology* (California: Elsevier Academic Press), 423, 549–572.
- Růžicka, K., Strader, L. C., Bailly, A., Yang, H., Blakeslee, J., Langowski, L., et al. (2010). Arabidopsis PIS1 encodes the ABCG37 transporter of auxinic compounds including the auxin precursor indole-3-butyric acid. *Proc. Natl. Acad. Sci.* 107, 10749–10753. doi: 10.1073/PNAS.1005878107
- Ryu, H., Kim, K., Cho, H., Park, J., Choe, S., and Hwang, I. (2007). Nucleocytoplasmic shuttling of BZR1 mediated by phosphorylation is essential in Arabidopsis Brassinosteroid signaling. *Plant Cell* 19, 2749–2762. doi: 10.1105/TPC.107.053728
- Sakai, H., Aoyama, T., and Oka, A. (2000). Arabidopsis ARR1 and ARR2 response regulators operate as transcriptional activators. *Plant J.* 24, 703–711. doi: 10.1046/j.1365-313X.2000.00909.x
- Scardoni, G., Petterlini, M., and Laudanna, C. (2009). Analyzing biological network parameters with CentiScaPe. *Bioinformatics* 25, 2857–2859. doi: 10.1093/bioinformatics/btp517
- Schaller, G. E., Bishopp, A., and Kieber, J. J. (2015). The yin-yang of hormones: cytokinin and auxin interactions in plant development. *Plant Cell* 27, 44–63. doi: 10.1105/tpc.114.133595
- Schlegel, J., Denay, G., Pinto, K. G., Stahl, Y., Schmid, J., Blümke, P., et al. (2021). Control of Arabidopsis shoot stem cell homeostasis by two antagonistic CLE peptide signalling pathways. *bioRxiv* [preprint]. doi: 10.1101/2021.06.14.448384
- Shannon, P., Markiel, A., Ozier, O., Baliga, N. S., Wang, J. T., Ramage, D., et al. (2003). Cytoscape: a software environment for integrated models of biomolecular interaction networks. *Genome Res.* 13, 2498–2504. doi: 10.1101/gr.1239303
- Shen, L., Liang, Z., Gu, X., Chen, Y., Teo, Z. W. N., Hou, X., et al. (2016). N6-Methyladenosine RNA modification regulates shoot stem cell fate in Arabidopsis. *Dev. Cell* 38, 186–200. doi: 10.1016/j.devcel.2016.06.008
- Sheremet, Y. A., Yemets, A. I., Vissenberg, K., Verbelen, J. P., and Blume, Y. B. (2010). Effects of inhibitors of serine/threonine protein kinases on *Arabidopsis thaliana* root morphology and microtubule Organization in its Cells. *Cell Tissue Biol.* 4, 399–409. doi: 10.1134/S1990519X10040139
- Shi, B., Zhang, C., Tian, C., Wang, J., Wang, Q., Xu, T., et al. (2016). Two-step regulation of a Meristematic cell population acting in shoot branching in Arabidopsis. *PLoS Genet.* 12:e1006168. doi: 10.1371/journal.pgen.1006168
- Slavikova, S., Ufaz, S., Avin-Wittenberg, T., Levanony, H., and Galili, G. (2008). An autophagy-associated Atg8 protein is involved in the responses of Arabidopsis seedlings to hormonal controls and abiotic stresses. *J. Exp. Bot.* 59, 4029–4043. doi: 10.1093/JXB/ERN244
- Somssich, M., Je, B. I., Simon, R., and Jackson, D. (2016). CLAVATA-WUSCHEL signaling in the shoot meristem. *Development* 143, 3238–3248. doi: 10.1242/dev.133645
- Song, S. K., and Clark, S. E. (2005). POL and related phosphatases are dosage-sensitive regulators of meristem and organ development in Arabidopsis. *Dev. Biol.* 285, 272–284. doi: 10.1016/j.ydbio.2005.06.020
- Song, S.-K., Lee, M. M., and Clark, S. E. (2006). POL and PLL1 phosphatases are CLAVATA1 signaling intermediates required for Arabidopsis shoot and floral stem cells. *Development* 133, 4691–4698. doi: 10.1242/DEV.02652
- Song, S. K., Yun, Y. B., and Lee, M. M. (2020). POLTERGEIST and POLTERGEIST-LIKE1 are essential for the maintenance of post-embryonic shoot and root apical meristems as revealed by a partial loss-of-function mutant allele of pll1 in Arabidopsis. *Genes Genom.* 42, 107–116. doi: 10.1007/s13258-019-00894-8
- Stefano, G., Renna, L., Wormsbaecher, C., Gamble, J., Zienkiewicz, K., and Brandizzi, F. (2018). Plant endocytosis requires the ER membrane-anchored proteins VAP27-1 and VAP27-3. *Cell Rep.* 23, 2299–2307. doi: 10.1016/j.celrep.2018.04.091
- Stephenson, K., Yamaguchi, Y., and Hoch, J. A. (2000). The mechanism of action of inhibitors of bacterial two-component signal transduction systems \*. *J. Biol. Chem.* 275, 38900–38904. doi: 10.1074/JBC.M006633200
- Tan, S., Luschnig, C., and Ri Friml, J. (2021). Pho-view of Auxin: reversible protein phosphorylation in Auxin biosynthesis. *Transport Signal.* 14, 151–165. doi: 10.1016/j.molp.2020.11.004
- The Gene Ontology Consortium (2014). Gene ontology consortium: going forward. *Nucleic Acids Res.* 43, D1049–D1056. doi: 10.1093/nar/gku1179
- Trehin, C., Schrempp, S., Chauvet, A., Berne-Dedieu, A., Thierry, A.-M., Faure, J.-E., et al. (2013). QUIRKY interacts with STRUBBELIG and PAL OF QUIRKY to regulate cell growth anisotropy during Arabidopsis gynoecium development. *Development* 140, 4807–4817. doi: 10.1242/dev.091868

- Tyanova, S., Temu, T., and Cox, J. (2016a). The MaxQuant computational platform for mass spectrometry-based shotgun proteomics. *Nat. Protoc.* 11, 2301–2319. doi: 10.1038/nprot.2016.136
- Tyanova, S., Temu, T., Sinitcyn, P., Carlson, A., Hein, M. Y., Geiger, T., et al. (2016b). The Perseus computational platform for comprehensive analysis of (prote) omics data. *Nat. Methods* 13, 731–740. doi: 10.1038/nmeth.3901
- Vaddepalli, P., Herrmann, A., Fulton, L., Oelschner, M., Hillmer, S., Stratil, T. F., et al. (2014). The C2-domain protein QUIRKY and the receptor-like kinase STRUBBELIG localize to plasmodesmata and mediate tissue morphogenesis in *Arabidopsis thaliana*. *Development* 141, 4139–4148. doi: 10.1242/dev.113878
- Valvekens, D., Van Montagu, M., and Van Lijsebettens, M. (1988). Agrobacterium tumefaciens-mediated transformation of *Arabidopsis thaliana* root explants by using kanamycin selection. *Proc. Natl. Acad. Sci. U. S. A.* 85, 40–5536.
- Van Leene, J., Han, C., Gadeyne, A., Eeckhout, D., Matthijs, C., Cannoot, B., et al. (2019). Capturing the phosphorylation and protein interaction landscape of the plant TOR kinase. *Nat. Plants* 5, 316–327. doi: 10.1038/s41477-019-0378-z
- van Wijk, K. J., Friso, G., Walther, D., and Schulze, W. X. (2014). Meta-analysis of *Arabidopsis thaliana* phospho-proteomics data reveals compartmentalization of phosphorylation motifs. *Plant Cell* 26, 2367–2389. doi: 10.1105/tpc.114.125815
- Vert, G., Walcher, C. L., Chory, J., and Nemhauser, J. L. (2008). Integration of auxin and brassinosteroid pathways by Auxin response factor 2. *Proc. Natl. Acad. Sci.* 105, 9829–9834. doi: 10.1073/PNAS.0803996105
- Vu, L. D., Stes, E., Van Bel, M., Nelissen, H., Maddelein, D., Inzé, D., et al. (2016). Up-to-date workflow for plant (Phospho) proteomics identifies differential drought-responsive phosphorylation events in maize leaves. *J. Proteome Res.* 15, 4304–4317. doi: 10.1021/acs.jproteome.6b00348
- Wang, H., Chevalier, D., Larue, C., Cho, S. K., and Walker, J. C. (2007). The protein phosphatases and protein kinases of *Arabidopsis thaliana*. *Arab. B.* 5:e0106. doi: 10.1199/tab.0106
- Wang, X., Gingrich, D. K., Deng, Y., and Hong, Z. (2012). A nucleostemin-like GTPase required for normal apical and floral meristem development in *Arabidopsis*. *Mol. Biol. Cell* 23, 1446–1456. doi: 10.1091/MBC.E11-09-0797
- Wang, P., Hawkins, T. J., Richardson, C., Cummins, I., Deeks, M. J., Sparkes, I., et al. (2014a). The plant cytoskeleton, NET3C, and VAP27 mediate the link between the plasma membrane and endoplasmic reticulum. *Curr. Biol.* 24, 1397–1405. doi: 10.1016/j.cub.2014.05.003
- Wang, Z., Li, X., Liu, N., Peng, Q., Wang, Y., Fan, B., et al. (2019b). A family of NAL2-interacting proteins in the biogenesis of the ER body and related structures. *Plant Physiol.* 180, 212–227. doi: 10.1104/PP.18.01500
- Wang, P., Pleskot, R., Zang, J., Winkler, J., Wang, J., Yperman, K., et al. (2019a). Plant AtEH/Pan1 proteins drive autophagosome formation at ER-PM contact sites with actin and endocytic machinery. *Nat. Commun.* 10, 1–16. doi: 10.1038/s41467-019-12782-6
- Wang, X., Qi, M., Li, J., Ji, Z., Hu, Y., Bao, F., et al. (2014b). The phosphoproteome in regenerating protoplasts from *Physcomitrella patens* protonemata shows changes paralleling postembryonic development in higher plants. *J. Exp. Bot.* 65, 2093–2106. doi: 10.1093/jxb/eru082
- Wang, P., Richardson, C., Hawkins, T. J., Sparkes, I., Hawes, C., and Hussey, P. J. (2016). Plant VAP27 proteins: domain characterization, intracellular localization and role in plant development. *New Phytol.* 210, 1311–1326. doi: 10.1111/NPH.13857
- Wang, X., Xie, B., Zhu, M., Zhang, Z., and Hong, Z. (2011). Nucleostemin-like 1 is required for embryogenesis and leaf development in *Arabidopsis*. *Plant Mol. Biol.* 78, 31–44. doi: 10.1007/S11103-011-9840-7
- Welch, D., Hassan, H., Blilou, I., Immink, R., Heidstra, R., and Scheres, B. (2007). *Arabidopsis* JACKDAW and MAGPIE zinc finger proteins delimit asymmetric cell division and stabilize tissue boundaries by restricting SHORT-ROOT action. *Genes Dev.* 21, 2196–2204. doi: 10.1101/gad.440307
- Wildwater, M., Campilho, A., Perez-Perez, J. M., Heidstra, R., Blilou, I., Korthout, H., et al. (2005). The RETINOBLASTOMA-RELATED gene regulates stem cell maintenance in *Arabidopsis* roots. *Cell* 123, 1337–1349. doi: 10.1016/j.CELL.2005.09.042
- Wilson, R. C., and Doudna, J. A. (2013). Molecular mechanisms of RNA interference. *Annu. Rev. Biophys.* 42, 217–239. doi: 10.1146/ANNUREV-BIOPHYS-083012-130404
- Wu, X. N., Rodriguez, C. S., Pertl-Obermeyer, H., Obermeyer, G., and Schulze, W. X. (2013). Sucrose-induced receptor kinase SIRK1 regulates a plasma membrane aquaporin in *Arabidopsis*. *Mol. Cell. Proteomics* 12, 2856–2873. doi: 10.1074/MCP.M113.029579
- Xiong, Y., McCormack, M., Li, L., Hall, Q., Xiang, C., and Sheen, J. (2013). Glucose-TOR signalling reprograms the transcriptome and activates meristems. *Nature* 496, 181–186. doi: 10.1038/nature12030
- Xiong, Y., and Sheen, J. (2012). Rapamycin and glucose-target of Rapamycin (TOR) protein signaling in plants. *J. Biol. Chem.* 287, 2836–2842. doi: 10.1074/JBC.M111.300749
- Xuan, W., Murphy, E., Beekman, T., Audenaert, D., and De Smet, I. (2013). Synthetic molecules: helping to unravel plant signal transduction. *J. Chem. Biol.* 6, 43–50. doi: 10.1007/s12154-013-0091-8
- Xue, T., Dai, X., Wang, R., Wang, J., Liu, Z., and Xiang, F. (2017). ARGONAUTE10 inhibits in vitro shoot regeneration via repression of miR165/166 in *Arabidopsis thaliana*. *Plant Cell Physiol.* 58, 1789–1800. doi: 10.1093/pcp/pcx117
- Yu, L. P., Miller, A. K., and Clark, S. E. (2003). POLTERGEIST encodes a protein phosphatase 2C that regulates CLAVATA pathways controlling stem cell identity at *Arabidopsis* shoot and flower meristems. *Curr. Biol.* 13, 179–188. doi: 10.1016/S0960-9822(03)00042-3
- Zhang, L., Li, X., Li, D., Sun, Y., Li, Y., Luo, Q., et al. (2018). CARK1 mediates ABA signaling by phosphorylation of ABA receptors. *Cell Discov.* 4, 30–10. doi: 10.1038/s41421-018-0029-y
- Zhang, T.-Q., Lian, H., Zhou, C.-M., Xu, L., Jiao, Y., and Wang, J.-W. (2017). A two-step model for de novo activation of WUSCHEL during plant shoot regeneration. *Plant Cell Online* 29, 1073–1087. doi: 10.1105/tpc.16.00863
- Zhang, Y., Xiao, Y., Du, F., Cao, L., Dong, H., and Ren, H. (2011). *Arabidopsis* VILLIN4 is involved in root hair growth through regulating actin organization in a Ca<sup>2+</sup>-dependent manner. *New Phytol.* 190, 667–682. doi: 10.1111/j.1469-8137.2010.03632.x
- Zhang, Z., and Zhang, X. (2012). Argonautes compete for miR165/166 to regulate shoot apical meristem development. *Curr. Opin. Plant Biol.* 15, 652–658. doi: 10.1016/j.PBI.2012.05.007
- Zhang, Y., Zheng, L., Hong, J. H., Gong, X., Zhou, C., Pérez-Pérez, J. M., et al. (2016). TOPOISOMERASE1 $\alpha$  acts through two distinct mechanisms to regulate stele and Columella stem cell maintenance. *Plant Physiol.* 171, 483–493. doi: 10.1104/PP.15.01754
- Zhou, Y., Honda, M., Zhu, H., Zhang, Z., Guo, X., Li, T., et al. (2015). Spatiotemporal sequestration of miR165/166 by *Arabidopsis* Argonaute10 promotes shoot apical meristem maintenance. *Cell Rep.* 10, 1819–1827. doi: 10.1016/j.CELREP.2015.02.047
- Zhu, H., Hu, F., Wang, R., Zhou, X., Sze, S. H., Liou, L. W., et al. (2011). *Arabidopsis* Argonaute10 specifically sequesters miR166/165 to regulate shoot apical meristem development. *Cell* 145, 242–256. doi: 10.1016/j.CELL.2011.03.024
- Zhu, T., Li, L., Feng, L., Mo, H., and Ren, M. (2020a). Target of Rapamycin regulates genome methylation reprogramming to control plant growth in *Arabidopsis*. *Front. Genet.* 11:186. doi: 10.3389/fgene.2020.00186
- Zhu, Y., Orre, L. M., Tran, Y. Z., Mermelekas, G., Johansson, H. J., Malyutina, A., et al. (2020b). DEqMS: A method for accurate variance estimation in differential protein expression analysis \*. *Mol. Cell. Proteomics* 19, 1047–1057. doi: 10.1074/MCP.TIR119.001646
- Li, Z.-Y., Xu, Z.-S., He, G.-Y., Yang, G.-X., Chen, M., Li, L.-C., et al. (2012). A mutation in *Arabidopsis* BSK5 encoding a brassinosteroid-signaling kinase protein affects responses to salinity and abscisic acid. *Biochem. Biophys. Res. Commun.* 426, 522–527. doi: 10.1016/j.BBRC.2012.08.118